

GEOSPHERE, v. 14, no. 3

<https://doi.org/10.1130/GES01617.1>

8 figures; 1 supplemental file

CORRESPONDENCE: portner@email.arizona.edu

CITATION: Portner, D.E., Delph, J.R., Biryol, C.B., Beck, S.L., Zandt, G., Özacar, A.A., Sandvol, E., and Türkelli, N., 2018, Subduction termination through progressive slab deformation across Eastern Mediterranean subduction zones from updated P-wave tomography beneath Anatolia: *Geosphere*, v. 14, no. 3, p. 907–925, <https://doi.org/10.1130/GES01617.1>.

Science Editor: Raymond M. Russo
Guest Associate Editor: Christian Teyssier

Received 27 September 2017
Revision received 3 February 2018
Accepted 9 April 2018
Published online 9 May 2018



This paper is published under the terms of the CC-BY-NC license.

© 2018 The Authors

Subduction termination through progressive slab deformation across Eastern Mediterranean subduction zones from updated P-wave tomography beneath Anatolia

Daniel Evan Portner¹, Jonathan R. Delph², C. Berk Biryol³, Susan L. Beck¹, George Zandt¹, A. Arda Özacar⁴, Eric Sandvol⁵, and Niyazi Türkelli⁶

¹Department of Geosciences, University of Arizona, Tucson, Arizona 85721, USA

²Department of Earth, Environmental, and Planetary Science, Rice University, Houston, Texas 77005, USA

³Department of Geological Sciences, University of North Carolina, Chapel Hill, North Carolina 27599, USA

⁴Department of Geological Engineering, Middle East Technical University, 06800 Ankara, Turkey

⁵Department of Geological Sciences, University of Missouri, Columbia, Missouri 65211, USA

⁶Kandilli Observatory and Earthquake Research Institute, Department of Geophysics, Boğazici University, 34684 Istanbul, Turkey

ABSTRACT

Using finite-frequency teleseismic P-wave tomography, we developed a new three-dimensional (3-D) velocity model of the mantle beneath Anatolia down to 900 km depth that reveals the structure and behavior of the subducting African lithosphere beneath three convergent domains of Anatolia: the Aegean, Cyprean, and Bitlis-Zagros domains. The Aegean slab has a relatively simple structure and extends into the lower mantle; the Cyprean slab has a more complex structure, with a western section that extends to the lower mantle with a consistent dip and an eastern section that is broken up into several pieces; and the Bitlis slab appears severely deformed, with only fragments visible in the mantle transition zone and uppermost lower mantle. In addition to the subducting slabs, high-amplitude slow velocity anomalies are imaged in the shallow mantle beneath recently active volcanic centers, and a prominent fast velocity anomaly dominates the shallow mantle beneath northern Anatolia and the southern Black Sea. As a whole, our model confirms the presence of well-established slow and fast velocity anomalies in the upper mantle beneath Anatolia and motivates two major findings about Eastern Mediterranean subduction: (1) Each of the slabs penetrates into the lower mantle, making the Eastern Mediterranean unique within the Mediterranean system, and (2) the distinct character of each slab segment represents different stages of subduction termination through progressive slab deformation. Our findings on the destructive processes of subduction termination and slab detachment have significant implications for understanding of the postdetachment behavior of subducted lithosphere.

INTRODUCTION

The interpretation of fast seismic velocity anomalies as subducted lithosphere from images in the lower mantle using seismic tomography is frequently used to inform tectonic reconstructions of past subduction and infer

properties of mantle dynamics such as slab sinking rates, lower-mantle viscosity, and ambient mantle flow (Van der Voo et al., 1999a; Hafkenscheid et al., 2006; Sigloch et al., 2008; van der Meer et al., 2010; Domeier et al., 2016; Wu et al., 2016). Such interpretations assume that subducted lithosphere remains stiff for up to hundreds of millions of years as it descends in the mantle before settling at the core-mantle boundary in the “slab graveyard” (Wysession, 1996; Rao and Kumar, 2014). However, slabs do not always remain cohesive, but instead can tear and segment as they descend into the mantle (Wortel and Spakman, 2000; Nolet, 2009; Biryol et al., 2011). This process is particularly notable in regions of continental collision through slab detachment (von Blanckenburg and Davies, 1995; Van der Voo et al., 1999b; Duretz et al., 2014).

The Eastern Mediterranean marks a major transition in the character of African-Arabian-Eurasian convergence from collision-dominated convergence in the east to subduction-dominated convergence in the west, making it an ideal region in which to investigate slab deformation during the latter stages of subduction. With this paper, we present some of the best-resolved seismic images to date of the Eastern Mediterranean subduction zones down to 900 km depth using a composite seismic array that includes data from the recent Continental Dynamics–Central Anatolian Tectonics (CD-CAT) seismic deployment in central Anatolia. Driven by these new images, we interpret the character of the modern subducted lithosphere beneath the entire Anatolian subcontinent in the context of Anatolian tectonics and discuss its implications for the fate of slabs in the mantle.

Tectonic Background

Anatolia formed from the amalgamation of major lithospheric blocks during a long history of Tethyan subduction that dates back at least to the Cretaceous (Şengör and Yılmaz, 1981; Menant et al., 2016; van Hinsbergen et al., 2016). Today, Anatolia is in a complex tectonic regime that can be described in three discrete neotectonic regions: the East Anatolian Contractual Prov-

ince, the West Anatolian Extensional Province, and the Central Anatolian Province (Şengör et al., 1985). These neotectonic regions roughly correlate with the three convergent domains used later herein to describe our results: the Bitlis-Zagros domain, the Aegean domain, and the Cyprean domain (Fig. 1).

In eastern Anatolia, the Bitlis-Zagros suture zone marks the modern boundary between the Arabian and Eurasian plates (Fig. 1). The Bitlis-Zagros suture zone formed in the mid-Miocene when the Arabian and Eurasian plates collided upon closure of the southern branch of the Neo-Tethys ocean (Şengör and Yilmaz, 1981; Okay et al., 2010; Nouri et al., 2016). Around 11–10 Ma, following Arabian-Eurasian collision, steepening and delamination of the subducted Neo-Tethyan slab from beneath eastern Anatolia resulted in an overriding crust with a thin or missing mantle lithosphere (Şengör et al., 2003; Angus et al., 2006).

Subsequent detachment opened a slab window, allowing for the upwelling of hot, fertile asthenosphere beneath what is now the high-elevation East Anatolian Plateau (Keskin, 2003, 2007; Şengör et al., 2003). Asthenospheric upwelling led to late Miocene to recent broad, domal uplift (Şengör et al., 2003) and enriched-mantle volcanism across the plateau (Pearce et al., 1990; Keskin, 2003) and continues to support the undercompensated crust of the plateau (Özacar et al., 2010). Today, convergence continues at a rate of 15 mm/yr (Reilinger et al., 2006), which is accommodated both by north-south-oriented shortening (Şengör et al., 2003) and the westward extrusion of Anatolia along the North Anatolian and East Anatolian faults (Barka and Reilinger, 1997).

The modern tectonic regime in western Anatolia is controlled by subduction along the Aegean Trench. Since at least 35–30 Ma, the Aegean Trench

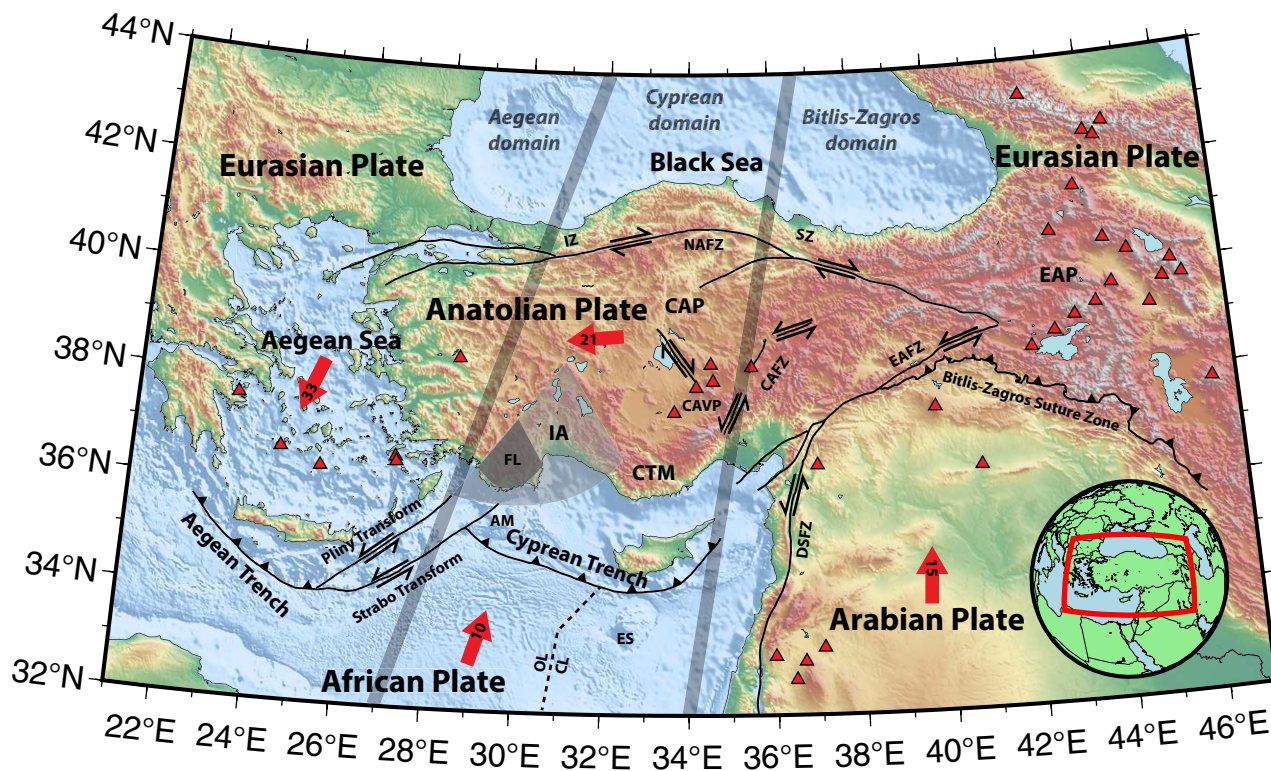


Figure 1. Topographic map with major tectonic features of the Anatolian region. Red arrows indicate plate motion, with velocities (on arrowheads, in mm/yr) and directions derived from global positioning system (GPS) measurements relative to stable Eurasia (Barka and Reilinger, 1997; Reilinger et al., 2006). Dashed line indicates boundary between subducting oceanic (OL) and continental lithosphere (CL; Granot, 2016). Black arrows indicate sense of shear along strike-slip faults. Red triangles indicate volcanoes active in the Holocene. Thick gray lines separate the three convergent domains listed from west to east: the Aegean domain, the Cyprean domain, and the Bitlis-Zagros domain. Abbreviations are as follows: AM—Anaximander Mountains; CAFZ—Central Anatolian fault zone; CAP—Central Anatolian Plateau; CAVP—Central Anatolian Volcanic Province; CTM—Central Taurus Mountains; DSFZ—Dead Sea fault zone; EAFZ—East Anatolian fault zone; EAP—East Anatolian Plateau; ES—Erathenes Seamount; FL—Fethiye Lobe; IA—Isparta angle; IZ—Istanbul zone; NAFZ—North Anatolian fault zone; SZ—Sakarya zone.

has migrated southward (Le Pichon and Angelier, 1979; Jolivet et al., 2013), contributing to extension in the overriding plate and thinning of the Aegean continental lithosphere. However, several mechanisms may contribute to extension, including trench migration, tectonic escape, and orogenic collapse (McKenzie, 1978; Şengör et al., 1985; Seyitoğlu and Scott, 1996; Reilinger et al., 2006; Jolivet et al., 2013). Today, the western Anatolian/Aegean crust is ~25–30 km thick (Zhu et al., 2006; Karabulut et al., 2013) after ~50% extension in the Aegean (McKenzie, 1978). An active arc and continuous Wadati-Benioff zone down to ~200 km depth (Papazachos et al., 2000) indicate continued active subduction along the Aegean Trench, while global positioning system (GPS) data indicate continued southward trench retreat (Reilinger et al., 2006).

Due to the Miocene collision of Arabia with Eurasia, the North Anatolian fault zone and conjugate faults in central-eastern Anatolia formed, accommodating westward extrusion and counterclockwise rotation of the Anatolian plate (Barka and Reilinger, 1997; Şengör et al., 2005). Deformation within central Anatolia is dominated by transtension, as expressed by increased exhumation rates and extensional basin formation related to the Central Anatolian fault zone (Koçyiğit and Beyhan, 1998; Fayon and Whitney, 2007; Higgins et al., 2015), which have facilitated the voluminous Miocene to recent volcanism of the Central Anatolian Volcanic Province (Toprak and Göncüoğlu, 1993; Toprak, 1998; Kuscu and Geneli, 2010) within the interior of the Central Anatolian Plateau. Conversely, the Central Taurus Mountains, which bound the southern margin of the Central Anatolian Plateau, have undergone little internal deformation since the mid-Miocene, despite ~2 km uplift since 8 Ma (Cosentino et al., 2012; Schildgen et al., 2012). Active deformation in central Anatolia occurs in the context of ongoing subduction along the Cyprean Trench. The Cyprean trench connects to the Aegean Trench to the west via the Pliny-Strabo subduction-transform edge propagator (STEP) system (Govers and Wortel, 2005) and to the Bitlis-Zagros suture to the east through the diffuse plate boundary beneath the Adana Basin (Abgarmi et al., 2017). The subducting material along the Cyprean trench is itself complex. The western edge of Cyprus marks a boundary between subducting continental lithosphere to the east and oceanic lithosphere to the west (Fig. 1; Granot, 2016). The arrival of two attenuated fragments of Gondwanan continental lithosphere, the Eratosthenes and Anaximander Seamounts, complicate subduction further (Fig. 1). The Eratosthenes Seamount is a Gondwana-derived rifted continental fragment actively underthrusting beneath Cyprus (Robertson, 1998) and potentially contributing to the shallow slab dip angle of the Cyprean slab (Biryol et al., 2011; Bakırcı et al., 2012). The Anaximander Mountains are being underthrust offshore of Anatolia's southwestern coast beneath the Isparta angle, which is a unique, largely undeforming, independently moving block separating the central Anatolian (Cyprean) and Aegean convergent domains (Barka and Reilinger, 1997; Zitter et al., 2003). While subduction of the Cyprean slab is a key control on the complexity of central Anatolian tectonics, a Wadati-Benioff zone that is largely restricted to the upper 100 km limits direct observations of Cyprean slab geometry.

Most attempts to understand the complex tectonics of Anatolia, as with the greater Mediterranean region, begin with African-Arabian subduction be-

neath Eurasia and its role in affecting mantle flow (Wortel and Spakman, 2000; Faccenna et al., 2014). For example, models proposed to explain the Eastern Anatolian and Central Anatolian Plateaus' kinematic, magmatic, and/or uplift history invoke a variety of mechanisms, including propagating slab detachment (Wortel and Spakman, 2000; Cosentino et al., 2012; Schildgen et al., 2012, 2014), slab rollback-related delamination (Göğüş and Psyklywec, 2008; van Hinsbergen et al., 2010; Bartol and Govers, 2014), multiple contemporaneous subduction zones (van Hinsbergen et al., 2016; Gürer et al., 2016), and slab-induced mantle convection (Faccenna and Becker, 2010; Reid et al., 2017). Each proposed mechanism makes predictions about the current structure of subducted Tethyan lithosphere and the surrounding mantle structure that can only be probed with seismic imaging techniques.

Previous Seismic Imaging

Several studies have investigated the seismic structure of the mantle beneath Anatolia at a variety of scales. Studies of the uppermost mantle show velocities slower than the global average across the entire region (Gans et al., 2009; Mutlu and Karabulut, 2011; Salaün et al., 2012; Delph et al., 2015a; Govers and Fichtner, 2016). Evidence from Pn tomography (Gans et al., 2009; Mutlu and Karabulut, 2011), surface wave tomography (Bakırcı et al., 2012; Salaün et al., 2012; Delph et al., 2017), teleseismic tomography (Biryol et al., 2011; Salah, 2017), ambient noise tomography (Warren et al., 2013), full-waveform tomography (Fichtner et al., 2013; Govers and Fichtner, 2016), and joint receiver function–surface wave dispersion inversion (Gök et al., 2007; Delph et al., 2015b) all suggests that velocities are particularly slow beneath eastern Anatolia throughout the upper mantle, supporting the hypothesis of rising hot asthenosphere through a slab window (Keskin, 2003; Şengör et al., 2003). Slow velocities as far west as the Isparta angle have been included with those beneath the East Anatolian Plateau to represent inflowing asthenosphere resulting from recent large-scale slab delamination and rollback beneath central and eastern Anatolia (Bartol and Govers, 2014; Govers and Fichtner, 2016).

The subducting Aegean and Cyprean slabs have also been imaged at a variety of scales beneath Turkey. The shallow slabs are thought to be separated by a vertical STEP-related tear approximately below the Isparta angle (de Boorder et al., 1998; Biryol et al., 2011; Salaün et al., 2012). While the Aegean slab appears to dip at a typical subduction angle at shallow depths (Salaün et al., 2012), the Cyprean slab appears to subduct subhorizontally as far north as 38°N (Bakırcı et al., 2012; Abgarmi et al., 2017; Delph et al., 2017). Regional- and global-scale body wave tomography images show both slabs continuing through the mantle transition zone, where they appear to connect, thicken, and temporarily flatten (Bijwaard et al., 1998; Piromallo and Morelli, 2003; Biryol et al., 2011). However, while the Aegean slab appears continuous with a near-constant dip through the upper mantle in most models, the Cyprean slab anomaly appears more diffuse and irregular, suggesting the slab may be

actively deforming and segmenting as it subducts (Biryol et al., 2011). Upon flattening in the mantle transition zone (Biryol et al., 2011), both slabs appear to continue into the lower mantle (Bijwaard et al., 1998; Piromallo and Morelli, 2003) as a result of the accumulation of a critical mass of oceanic lithosphere (Faccenna et al., 2003).

The abundance of seismic research in Anatolia provides an excellent framework within which to view the general character of Eastern Mediterranean slabs from the surface into the lower mantle, but methodological and data limitations in these studies inhibit their ability to resolve the finer-scale structure of the various slab segments beneath Anatolia, which are critical to evaluating the tectonic and geodynamic evolution of the Eastern Mediterranean system. More recent regional body wave tomography has improved upon this with the incorporation of frequency-dependent sensitivity kernels and a denser seismic network, providing images of tears within a once-continuous Tethyan slab and revealing the segmented nature of the subducting Cyprean slab (Biryol et al.,

2011). However, this model lacks the resolution in central Turkey to delineate the structure, deformation, and segmentation of the Cyprean slab due to relatively sparse station density in the region at the time of the study. The model presented in this paper builds on the work of Biryol et al. (2011) through the addition of a dense data set in central Turkey and incorporation of data from the largely expanded national seismic network in Turkey (Fig. 2), allowing us to obtain a detailed image of the structure of the Cyprean slab and surrounding slabs down to 900 km depth.

DATA AND METHODS

The tomography model presented here serves as a significant update on the tomography model of Biryol et al. (2011). Next, we briefly review the data and methodology used in these studies while highlighting the relevant modi-

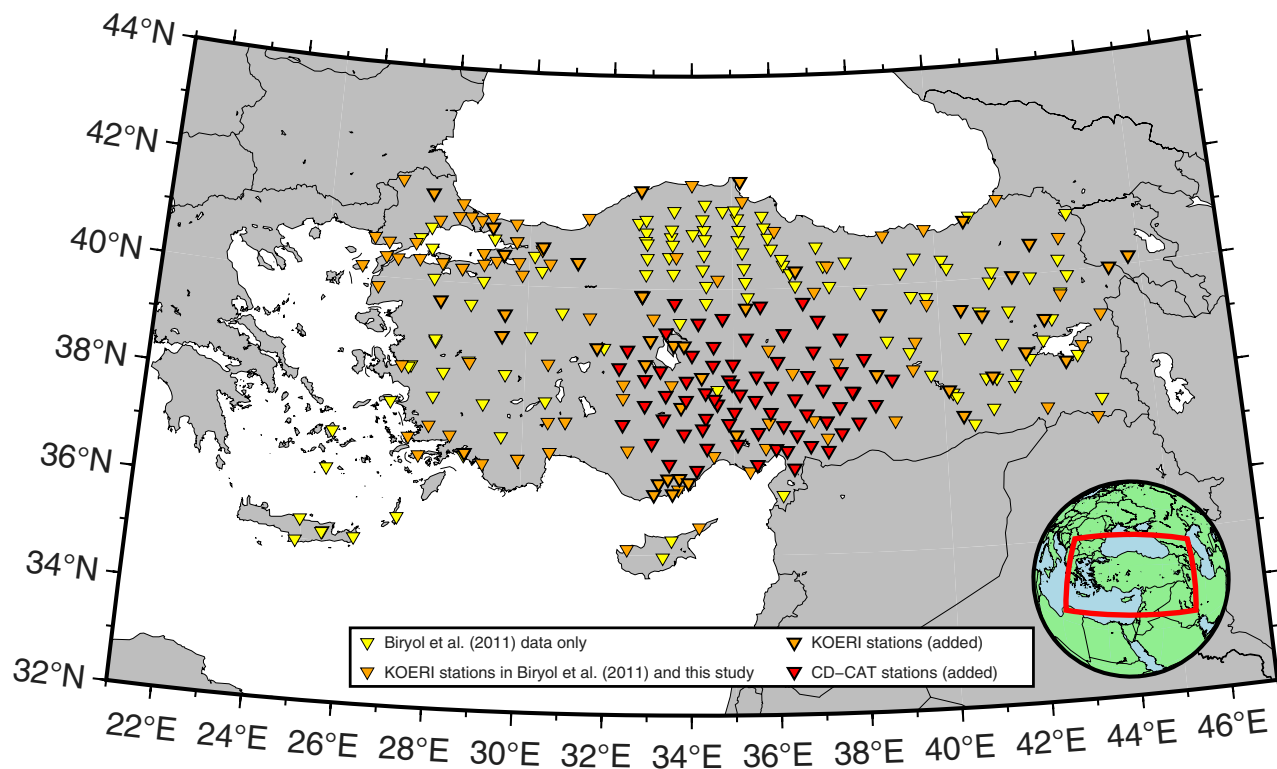


Figure 2. Map of seismic stations used in this study. Yellow and orange triangles without a bold outline indicate stations that were included in the original data set of Biryol et al. (2011), while orange and red triangles with bold outlines are new to the data set. Orange triangles without a bold outline indicate stations that were included in the original data set but data between 2013 and 2015 were added for the present study. KOERI—Kandilli Observatory Digital Broadband Seismic Network; CD-CAT—Continental Dynamics—Central Anatolian Tectonics Project.

fifications made for the current study. For a more detailed description of the methodology and its limitations, see Biryol et al. (2011) and Schmandt and Humphreys (2010).

Data

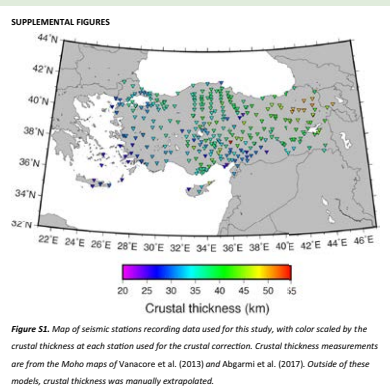
For this study, we utilized the data set of Biryol et al. (2011), which consists of 33,990 direct P and PKIKP phase arrival times from 409 unique earthquakes recorded at a variety of temporary (Sandvol, 1999; Mitchell and Zhu, 2002; Beck and Zandt, 2005) and permanent (Albuquerque Seismological Laboratory [ASL]/USGS, 1988; GEOFON Data Centre, 1993; Bogazici University Kandilli Observatory and Earthquake Research Institute, 2001) seismic networks. Arrival times in that study were picked on seismograms filtered in three frequency bands with corner frequencies of 0.2–0.8 Hz, 0.1–0.4 Hz, and 0.04–0.16 Hz for broadband stations and one frequency band with corner frequencies of 0.5–1.5 Hz for short-period stations.

We added data collected between 2013 and 2015 across two broadband seismic networks: the recent CD-CAT Project (72 stations; Sandvol, 2013) seismic array, and the Kandilli Observatory Digital Broadband Seismic Network (KOERI; 121 stations; Bogazici University Kandilli Observatory and Earthquake Research Institute, 2001; see Fig. 2). We picked arrivals from earthquakes with magnitude 5.0 and greater at distances between 30° and 90° from the stations for direct P phases (509 earthquakes) and between 155° and 180° from the stations for PKIKP phases (18 earthquakes; Fig. 3A). An excess of earthquakes from the west Pacific subduction zones led to an uneven back-azimuthal distribution

(Fig. 3B), so to more evenly distribute the back-azimuthal distribution of rays, we excluded from our data set ~47,000 rays from earthquakes in the west Pacific by preferentially removing earthquakes with fewer recovered residuals. Arrival times were picked on seismograms filtered in four frequency bands with corner frequencies of 0.5–1.5 Hz, 0.2–0.8 Hz, 0.1–0.4 Hz, and 0.04–0.16 Hz for all stations. After combining data sets, we used 66,331 arrival times (12% from bandpass 0.5–1.5 Hz, 34% from bandpass 0.2–0.8 Hz, 31% from bandpass 0.1–0.4 Hz, and 23% from bandpass 0.04–0.16 Hz), consisting of 65,352 direct phases and 979 core phases from 936 earthquakes over the time period between 1999 and 2015.

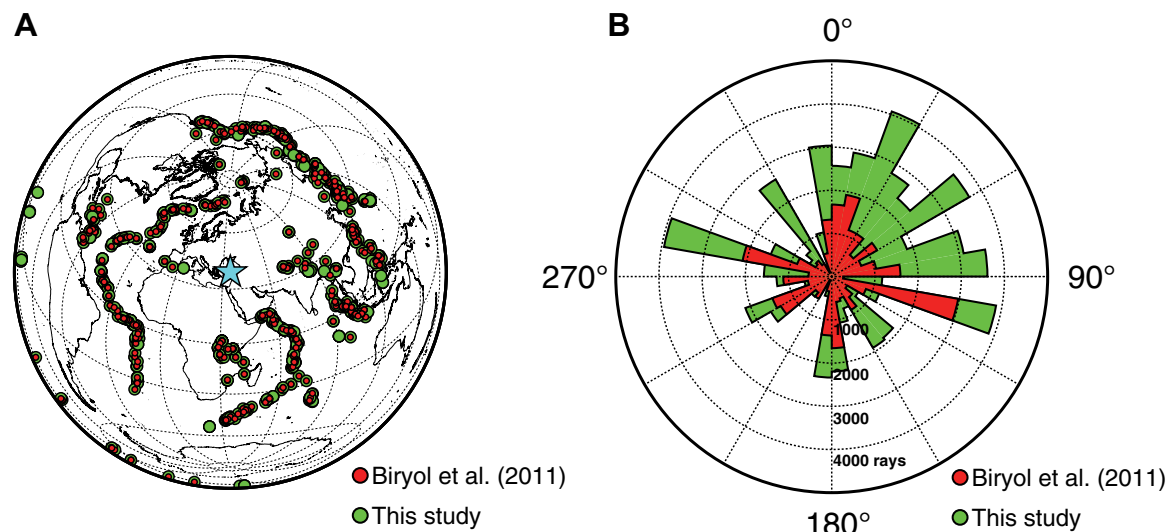
Traveltime Residuals

To obtain traveltime residuals, we used a multichannel cross-correlation algorithm (VanDecar and Crosson, 1990; Pavlis and Vernon, 2010). Relative traveltimes were determined with respect to the IASP91 one-dimensional (1-D) P-wave velocity model (Kennett and Engdahl, 1991) and de-meaned for each event. We additionally made a correction to the traveltime residual for crustal thickness beneath each station by assuming a vertical ray and constant velocity of 6.2 km/s in the lower crust. Crustal thicknesses were determined using the Moho map of Vanacore et al. (2013) and adjusted with more recent constraints from Abgarmi et al. (2017); see Supplemental Figure S1'. Outside of these models, crustal thickness was manually extrapolated. Notably, the crustal correction had negligible effect on the resulting model. Average traveltime residuals for each station are summarized in Figure 4.



Supplemental Material. Figures (S1) crustal thickness map, (S2) tradeoff analysis, (S3) hit quality maps, (S4) average velocity perturbations by layer, (S5) checkerboard analysis 3 in map view, (S6) checkerboard analysis in cross section, (S7) synthetic recovery test 1, (S8) synthetic recovery test 2, (S9) synthetic recovery test 3, (S10) noise recovery test, (S11) results in map view with discrete color scale, and (S12) results in cross section with discrete color scale. Please visit <https://doi.org/10.1130/GES01617.S1> or the full-text article on www.gsapubs.org to view the Supplemental Material.

Figure 3. (A) Earthquakes used for this study, with the complete data set (green) compared to the data included from Biryol et al. (2011; red) in relation to the study area (blue star). Core phases were picked from earthquakes at distances of 155° to 180°, while direct phases were picked from earthquakes at distances of 30° to 90°. (B) Back-azimuthal distribution of incoming rays, from the data set of Biryol et al. (2011; red) and the combined data set (green). Ray paths are dominated by the large number of earthquakes in the western Pacific subduction zones.



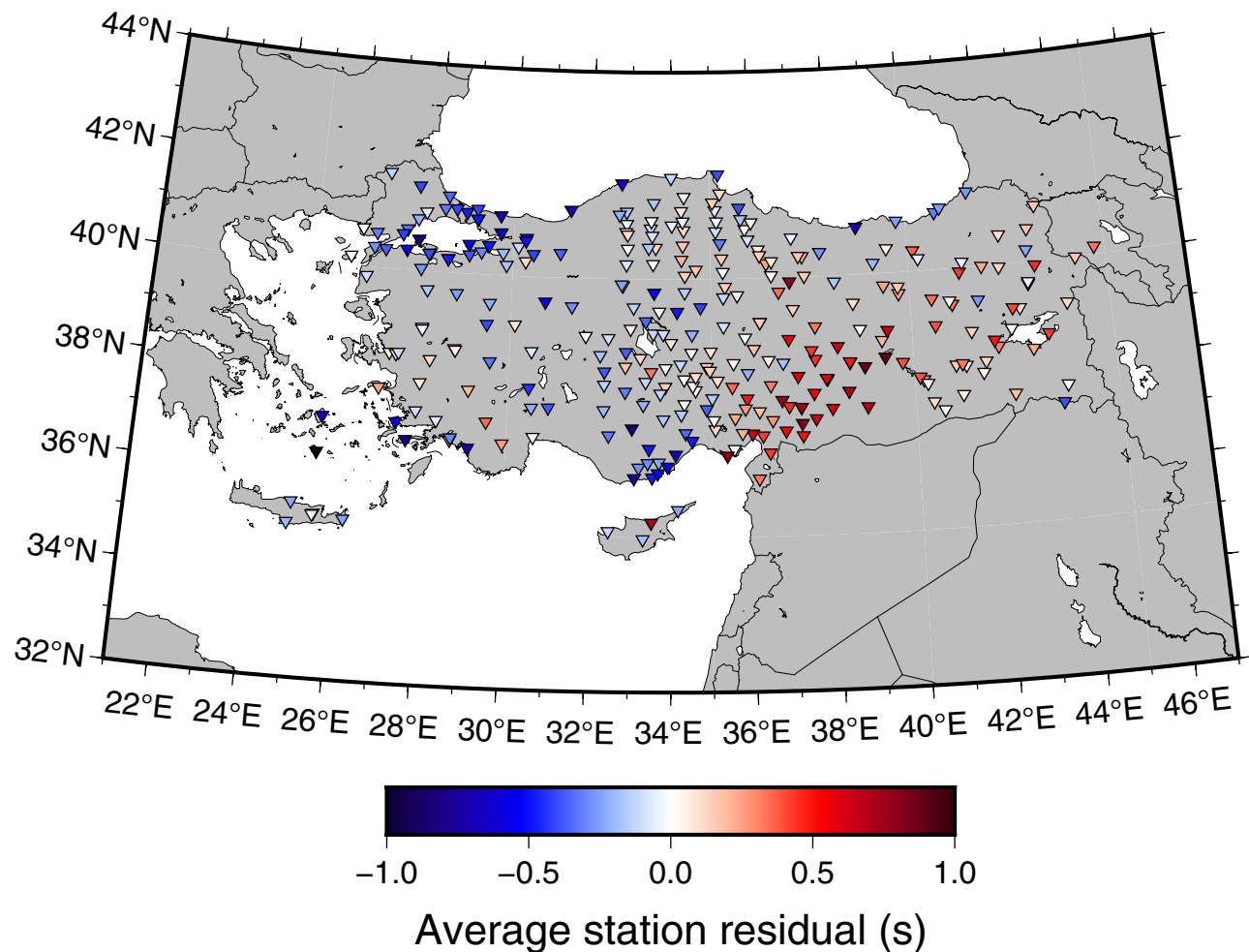


Figure 4. Map of stations used for this study, with color scaled by the average traveltime residual for that station. Traveltime residuals were determined after crustal thickness corrections. Note the relative delays in the east compared to early arrivals in western and central Anatolia, indicating slower velocities beneath eastern Anatolia.

Tomography Inverse Method

The method used in this study was the finite-frequency teleseismic tomography method (Dahlen et al., 2000; Schmandt and Humphreys, 2010). The finite-frequency method accounts for the frequency-dependent volumes surrounding the geometric ray path that are sampled by any given ray by approximating sensitivity with the Born theoretical “banana-doughnut” kernels for the first Fresnel zone (Dahlen et al., 2000). The inversion is a smoothed, damped

least-squares inversion to account for uncertainty in ray geometry and to regularize the inversion. Trade-off analysis indicates that a range of damping and smoothing parameters are justified (Fig. S2 [footnote 1]). We chose to adopt damping and smoothing parameters of 6 and 7, respectively, in accordance with the study of Biryol et al. (2011), for consistency and to facilitate comparison. Station and event terms were additionally included in the inversion to account for small-scale heterogeneity unaccounted for by our model geometry, such as local site effects.

The most significant changes to the Biryol et al. (2011) approach were in model space parameterization. The modeled region is 3300 km (E-W) by 2300 km (N-S) centered on 39°N, 35°E, with horizontal node spacing at the surface ranging from 35 km in the center to 56 km on the edges and dilating with depth to a maximum spacing ranging from 55 to 90 km at the base of the model space. Vertically, the model space extends from 60 km depth to 1010 km depth, with spacing ranging from 35 km near the surface to 70 km at the bottom. This is in contrast to Biryol et al. (2011), which extended from 35 km to 655 km. Model parameterization was chosen to optimize crossing-ray density as determined by hit quality, which quantitatively assesses the quantity and back-azimuthal distribution of rays sampling a given node (Schmandt and Humphreys, 2010; Biryol et al., 2011). The inclusion of 32,341 additional arrival times, primarily from the CD-CAT seismic array in central Anatolia, served to most significantly improve sampling of the upper mantle beneath central Anatolia and the transition zone and uppermost lower mantle across the study area, while having a minor effect on sampling of the upper mantle beneath western and eastern Anatolia (Fig. S3 [footnote 1]). This new data allowed our modeled region to have sufficient hit quality (hit quality > 0.5) within the lower mantle to justify extending the model space to 1010 km depth (Fig. S3G [footnote 1]). However, various tests suggest that the deepest two layers of the model space exhibit artificially high-amplitude velocity perturbations (Fig. S4 [footnote 1]); thus, we only interpreted results to 900 km depth.

RESULTS

Model Quality

Data variance reduction is a commonly used metric to assess the fit of a model to the data for the tomographic inverse problem. For this study, we obtained a variance reduction of 70%. However, while variance reduction indicates fit to the data, there is no such quantitative indicator for uncertainty. Instead, we performed a series of synthetic anomaly recovery tests to qualitatively assess uncertainty and the model's ability to recover structure.

First, we performed a standard checkerboard analysis, using alternating square synthetic input anomalies of $\pm 5\%$ separated by neutral zones of the same size (Figs. S5 and S6 [footnote 1]). On average, the checkerboard structure is well recovered beneath Turkey, where up to 50% of checker amplitude is recovered. Nonzero amplitude recovery in neutral input layers (Fig. S5C [footnote 1]) implies some degree of vertical smearing, while amplitude recovery between checkers indicates some lateral smearing induced by the smoothness constraint. Outside of Turkey (including beneath the Aegean Sea, the Black Sea, the Mediterranean Sea, and the Arabian plate), the checkerboard recovery drops significantly. In general, we found that anomaly geometry was recovered within the 0.5 hit quality contour, so we used this quantity to outline the well-resolved portion of our model in the results. However, this outline is not a deciding factor for model resolution; it was instead used as a proxy for the well-sampled portions of the model space.

Finally, in addition to the standard checkerboard analysis, isolated anomaly recovery tests were performed to assess the potential of our model to resolve synthetic structures and their geometries within the well-sampled portion of the model space (Figs. S7, S8, S9, and S10 [footnote 1]). These recovery tests are described in the discussion section.

Mantle P-Wave Velocity Model

The bulk character of the tomography model (Fig. 5) indicates dominantly slow velocity perturbations throughout the upper mantle, consistent with previous imaging efforts (Gans et al., 2009; Salaün et al., 2012; Delph et al., 2015a; Govers and Fichtner, 2016). These slow velocity perturbations grade into dominantly fast velocity perturbations below 500 km depth. Images of the tomography model are shown in Figures 6 and 7, as well as with a discrete color scale in Figures S11 and S12 (footnote 1). Several prominent velocity anomalies stand out in the upper mantle: a fast velocity anomaly parallel to the

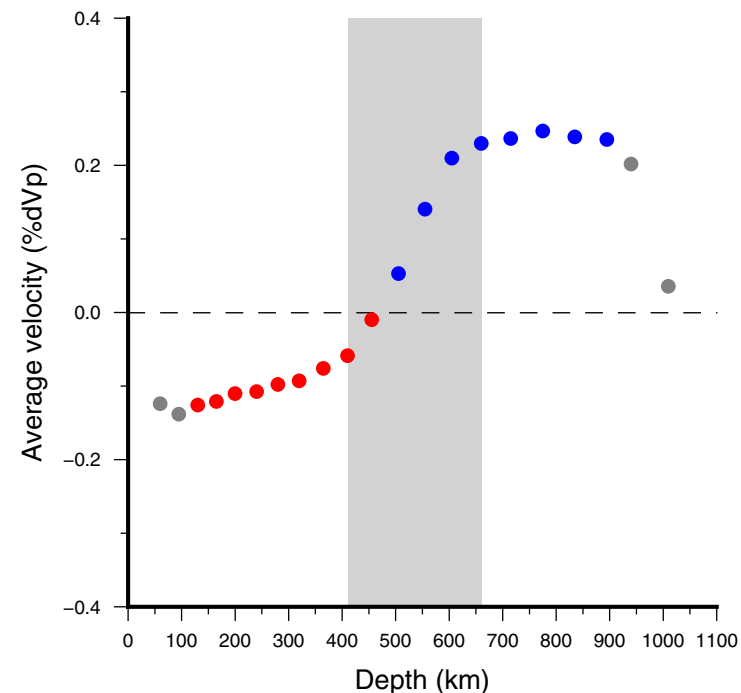


Figure 5. Average P-wave velocity perturbation for nodes with a hit quality >0.5 in each layer of the tomography model. Blue points represent fast average velocities, and red points represent slow average velocities. Gray points represent uninterpreted layers. The shaded region demarcates the mantle transition zone. Note that velocities are generally relatively slow in the upper mantle and fast in the lower mantle.

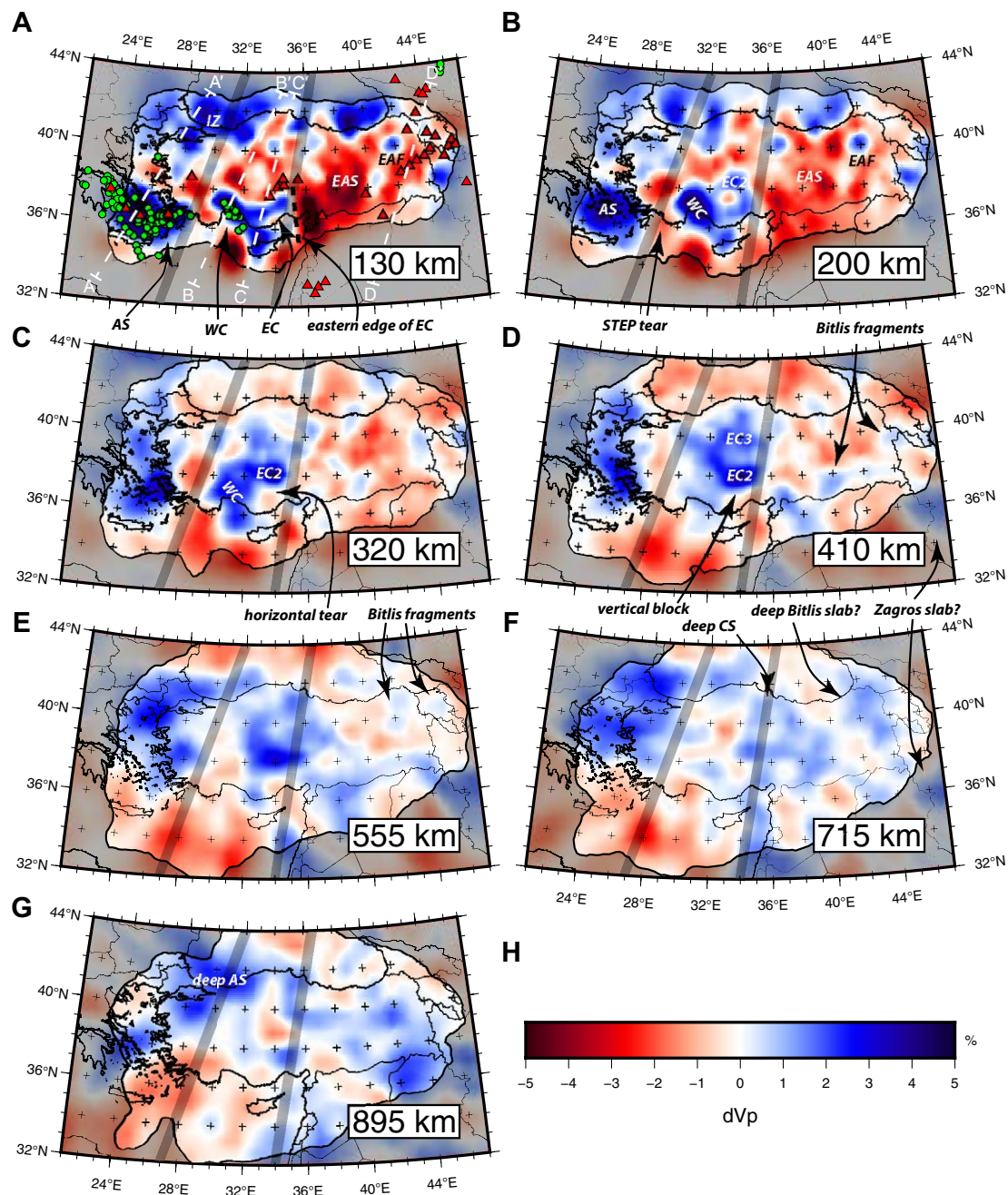


Figure 6. Results from the tomographic inversion at depths of (A) 130 km, (B) 200 km, (C) 320 km, (D) 410 km, (E) 555 km, (F) 715 km, and (G) 895 km. (H) Color scale for P-wave velocity perturbations. The dashed white lines in A indicate the locations of the cross sections in Figure 7. Solid black line surrounded by dark shading represents the 0.5 hit quality contour. Green circles are earthquake locations from the U.S. Geological Survey Advanced National Seismic System (ANSS) Comprehensive Earthquake Catalog (ComCat). As in Figure 1, red triangles indicate volcanoes active in the Holocene, and thick gray lines separate the three convergent domains. Abbreviations are as follows: AS—Aegean slab; CS—Cyprean slab; EAF—East Anatolian fast anomaly; EAS—East Anatolian slow anomaly; EC—east Cyprean slab; IZ—Istanbul Zone; STEP—subduction-transform edge propagator system; WC—west Cyprean slab.

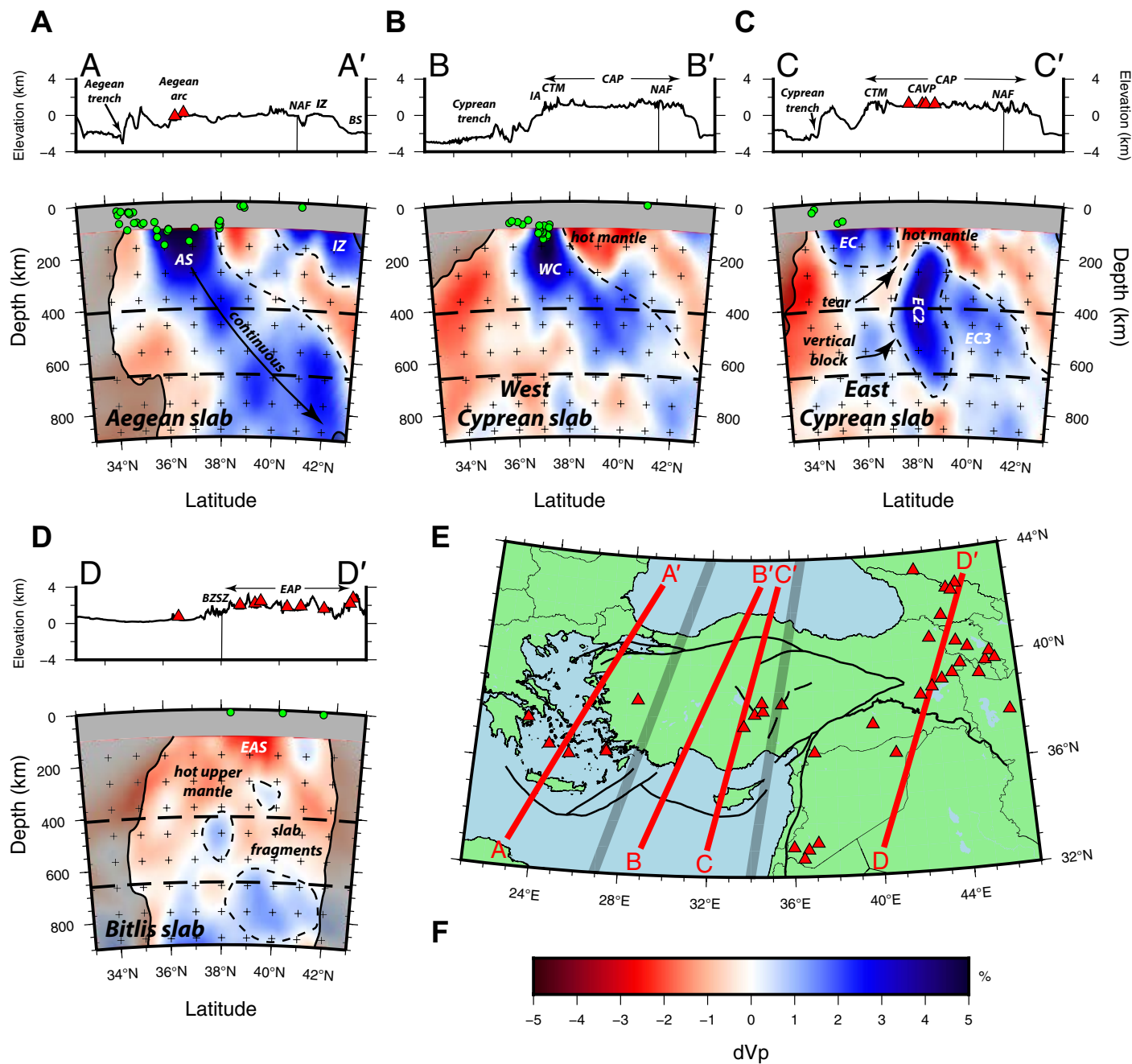


Figure 7. Cross sections through the tomography model at locations oriented down-dip of the (A) Aegean slab, (B) west Cyprean slab, (C) east Cyprean slab, and (D) Bitlis-Zagros suture zone. Topography and tectonic features are labeled above the profiles. (E) Map indicating the surface traces of the cross sections. Volcanoes and convergent domains are as in Figures 1 and 4. (F) Color scale for P-wave velocity perturbations. Dashed lines represent interpreted anomaly delineation. Abbreviations are as follows: AS—Aegean slab; BS—Black Sea; BZSZ—Bitlis-Zagros suture zone; CAP—Central Anatolian Plateau; CAVP—Central Anatolian Volcanic Province; CTM—Central Taurus Mountains; EAP—East Anatolian Plateau; EAS—East Anatolian slow anomaly; EC—east Cyprean slab; IA—Isparta angle; IZ—Istanbul zone; NAF—North Anatolian fault; WC—west Cyprean slab.

Aegean trench (labeled Aegean slab, or AS, in figures), a fast velocity anomaly north of the Cyprean trench (labeled WC and EC in figures), a slow velocity anomaly (labeled East Anatolian slow, or EAS, in figures) beneath the high elevations of eastern Anatolia, and a fast velocity anomaly (labeled as İstanbul zone, or IZ, in figures) underlying the İstanbul zone and the Pontide block in northern Anatolia. These prominent anomalies give way to interconnected low-amplitude fast velocity anomalies in the lower mantle across the whole region. To more clearly illustrate the three-dimensional (3-D) geometries of each of these anomalies, we present further descriptions of the model in three separate convergent domains, here listed from west to east: the Aegean domain, the Cyprean domain, and the Bitlis-Zagros domain.

In the Aegean domain, the most prominent anomaly is the fast velocity anomaly coincident with the Aegean Wadati-Benioff zone, anomaly AS (Figs. 6 and 7). However, while Wadati-Benioff zone earthquakes terminate at ~200 km depth (Papazachos et al., 2000), anomaly AS extends to the base of the model domain at 900 km depth, with a regular dip of ~60° toward the northeast (Fig. 7A). Anomaly AS has a reduced amplitude (average velocity perturbation ~1%) between 300 and 400 km depth before widening in the transition zone and uppermost lower mantle.

The Cyprean domain is dominated by a fast velocity anomaly to the north of the Cyprean trench that is distinct from the fast velocity anomaly in the Aegean domain, separated by vertically extensive slow velocities (labeled STEP tear in Fig. 6B). We refer to this as the Cyprean slab anomaly (labeled as EC and WC in Figs. 6, 7B, and 7C). The character of the Cyprean slab anomaly varies from west to east. The western part of the Cyprean anomaly (anomaly WC) coincides with Wadati-Benioff zone earthquakes that extend to ~150 km depth. Anomaly WC dips regularly to the northeast with high amplitude (average velocity perturbation ~3%) in the upper mantle (Fig. 7B). Upon reaching the transition zone, the amplitude of the anomaly is significantly reduced to ~2%, and the anomaly widens to the north by ~200 km. Low-amplitude fast velocity anomalies in the uppermost lower mantle beneath the Cyprean slab appear to be connected to the anomaly in the transition zone. Conversely, the eastern part of the Cyprean fast velocity anomaly (anomaly EC) directly north of Cyprus extends northward to ~37.5°N and in depth from the model surface to 200 km at a subhorizontal angle (Fig. 7C). Approximately 50 km to the north, there is a high-amplitude (average velocity perturbation ~3%), subvertically dipping, fast velocity anomaly (anomaly EC2) that extends from 200 km to 700 km depth. In cross section, this block appears separated from anomaly EC by low-amplitude slow velocities. While the amplitude of the intervening slow velocities is low (<1%), synthetic recovery tests indicate that significant separation between EC and EC2 is necessary to allow for intervening slow velocities, suggesting the separation is robust (Fig. S8 [footnote 1]). Within the mantle transition zone, this large, vertically dipping anomaly appears connected to a more disparate, low-amplitude fast velocity anomaly (anomaly EC3; average velocity perturbation ~1.5%) extending to the north, as well as into the lower mantle. In the lower mantle, smaller fast velocity anomalies are scattered below the larger blocks. Notably, while the western and eastern

portions of the Cyprean slab anomaly display distinct character, they appear to be connected.

The Bitlis-Zagros domain (Fig. 7D) is almost completely dominated by slow velocity perturbations (anomaly EAS), particularly at depths above ~200 km (average velocity perturbation ~3%). One prominent exception is a small fast velocity anomaly (anomaly EAF), centered at 42°E, 40°N, that is ~100 km in diameter and extends from ~100 to 300 km depth (average velocity perturbation ~2%). Below 200 km depth, the amplitudes of slow velocity perturbations are significantly lower (average velocity perturbation ~1%; Fig. 7D). Below ~300 km, additional small, low-amplitude fast velocity anomalies (average velocity perturbation ~1%) appear scattered across the domain. Interconnected low-amplitude fast velocity anomalies (average velocity perturbation ~1.5%) are prevalent near the base of the model (Fig. 6G).

Across all three convergent domains at shallow depths, there is a prominent fast velocity anomaly (anomaly IZ) that extends below the İstanbul zone, the Pontide block, and the southern Black Sea (Fig. 6). Anomaly IZ (average velocity perturbation ~3%) exhibits variable amplitude and shape, but it extends vertically to ~200 km depth. Widespread slow velocity perturbations separate anomaly IZ from the shallow slab anomalies.

DISCUSSION

Model Comparison

Before discussing the implications of the new features imaged with this model, we confirm the consistency of our model with other published seismic models in the literature by identifying expected velocity anomalies in the model domain that have previously been deemed robust. The most obvious expected anomalies are fast velocity anomalies associated with Wadati-Benioff zone earthquakes. Wadati-Benioff zones extend within our study region down-dip from the Aegean Trench to ~200 km depth and from the Cyprean trench to ~100 km depth. As expected, earthquakes in both Wadati-Benioff zones fall within high-amplitude fast velocity anomalies in the tomography model (Fig. 6A) that we interpret as the Aegean and Cyprean slabs, respectively. From prior seismic tomography (Bijwaard et al., 1998; Piromallo and Morelli, 2003), the Aegean slab anomaly has been known to extend into the lower mantle to at least 1000 km depth (Faccenna et al., 2003), and the Cyprean slab has been seen to extend at least into the mantle transition zone, indicating that both slabs are aseismic at depth. Both observations are confirmed with our new model.

A second expected feature in the tomography model is the presence of widespread slow velocity anomalies throughout the uppermost mantle beneath Anatolia, with particularly slow velocities beneath eastern Anatolia (Gök et al., 2007; Gans et al., 2009; Biryol et al., 2011; Mutlu and Karabulut, 2011; Bakırcı et al., 2012; Salaün et al., 2012; Fichtner et al., 2013; Warren et al., 2013;

Delph et al., 2015a; Govers and Fichtner, 2016; Salah, 2017). At the regional scale, shallow slow velocities are typically explained by mantle upwelling in response to slab detachment in eastern Anatolia (Keskin, 2003; Şengör et al., 2003), drip-style lithospheric delamination in central Anatolia (Göğüş et al., 2017), or rollback-style lithospheric delamination across central and eastern Anatolia (Bartol and Govers, 2014) and western Anatolia (van Hinsbergen et al., 2010). This manifests at the surface in a number of young volcanic fields that show an asthenospheric contribution to their geochemical signatures, such as in the widespread volcanism across the East Anatolian Plateau (Pearce et al., 1990; Şengör et al., 2008), mafic volcanism in the Central Anatolian Volcanic Province (Reid et al., 2017), the Miocene–Pliocene Kirka-Afyon-Isparta volcanic field (Francalanci et al., 2000), and the Pliocene–Pleistocene Kula volcanic field (Richardson-Bunbury, 1996; Savaşçın and Oyman, 1998; Tokçaer et al., 2005; Dilek and Altunkaynak, 2009). Our model confirms the presence of slow velocities at shallow depths across the region (Fig. 6A), with particularly slow velocities beneath eastern Anatolia (Fig. 4).

A third expected feature is the shallow fast velocity anomaly observed at the northern edge of the model (anomaly IZ; Figs. 6A and 7A). A similar anomaly was present in previous regional P-wave (Biryol et al., 2011; Yanovskaya et al., 2016) and S-wave (Salaün et al., 2012; Bakırcı et al., 2012; Fichtner et al., 2013) tomographic velocity models. This is typically interpreted as the strong mantle lithosphere of the Black Sea (Jiménez-Munt et al., 2003; Yegorova et al., 2013), the Istanbul zone near the western Pontides (Biryol et al., 2011), and the Sakarya zone (Fig. 1) near the central Pontides (Fichtner et al., 2013). Alternatively, correlation of the anomaly's southern boundary with the Izmir-Ankara-Erzincan suture zone has led to the interpretation of the anomaly as a remnant of Neo-Tethys subduction (Pourteau et al., 2010; Salaün et al., 2012) and/or partly related to underthrusting of the crystalline Kirşehir block (Espurt et al., 2014). However, synthetic recovery tests (Fig. S7 [footnote 1]) indicate that our model is unable to distinguish additional details of the structure of the anomaly, so we refrain from interpreting its origin.

As a whole, the present model accordingly corroborates each of the aforementioned studies, showing fast velocity anomalies corresponding to the locations of expected subducting slabs, prevalent slow velocities throughout most of the upper mantle beneath eastern Anatolia and recently active volcanism in central and western Anatolia (Fig. 7D), and fast seismic velocities at shallow depths north of the Izmir-Ankara-Erzincan suture zone.

Slab Structure and Tectonics

Significant fast velocity anomalies are observed in the upper mantle with varying intensity and structure in each of the three convergent domains: the Aegean domain, the Cyprean domain, and the Bitlis-Zagros domain. Here, we present our interpretations of these fast velocity anomalies and their relationship to subducted African-Arabian lithosphere. Our interpretation of the subducted slab structure is summarized in Figure 8.

Aegean and Cyprean Slabs

Fast velocity anomaly AS is coincident with Wadati-Benioff zone earthquakes at shallow depths and extends to the base of our model at 900 km depth (Figs. 6 and 7). The slab appears as a high-amplitude fast velocity anomaly that is continuous from the shallowest layers in our model to the lower mantle. Besides the concave curvature of the Aegean slab at shallow depths, which is related to the shape of the trench, the slab appears to have an otherwise simple character, with a consistent dip through the mantle. In contrast, the subducting Cyprean slab can be described in two parts: the western Cyprean slab (Fig. 7B) and the eastern Cyprean slab (Fig. 7C). Along the western Cyprean trench, where oceanic lithosphere is entering the trench (Granot, 2016), the slab exhibits a simple geometry similar to the Aegean slab. Here, the slab appears to subduct continuously through the upper mantle with a dip of $\sim 45^\circ$ to the NE, coinciding with a clear Wadati-Benioff zone. However, along the eastern portion of the Cyprean trench, the complex geometry of the eastern slab may be a result of the underthrusting of attenuated continental lithosphere at the trench (Delph et al., 2017), such as the Eratosthenes Seamount (Robertson, 1998; Schattner, 2010). Not only did the impingement of the Eratosthenes Seamount on the trench contribute to recent uplift on Cyprus (Robertson, 1998), but the subduction of attenuated continental material along the Cyprean trench is well correlated with a region of relative aseismicity in the shallow slab and northward-directed subhorizontal subduction (anomaly EC) between longitudes 32°E and 34°E (Fig. 7C). While relatively poor resolution near the surface hinders our ability to image the shallow slab segment in detail, this result is consistent with previous seismic imaging studies sensitive to uppermost mantle velocity structure (Bakırcı et al., 2012; Abgarmi et al., 2017; Delph et al., 2017).

Our interpretation of the eastern Cyprean slab supports a buoyancy-driven slab deformation mechanism. The shallowly subducting slab segment is separated from a large vertically dipping block of the Cyprean slab (anomaly EC2) that appears to be connected to the western Cyprean slab in the mantle transition zone. If the shallow segment consists of subducted continental lithosphere while the separated block consists of the leading oceanic lithosphere, we would expect a discrepancy in buoyancy, leading to a difference in the dip of the slab segments. Separation of the two slab segments (Fig. 6C; Fig. S8 [footnote 1]) further implies that this buoyancy contrast recently induced horizontal tearing of the slab. We infer the tearing to be propagating from east to west, where it ends near the edge of the subducting continental material, in a similar fashion to what is observed elsewhere in the Mediterranean system (Wortel and Spakman, 2000). Such a tear, coupled with slab rollback, likely alters mantle flow, allowing for upwelling through the tear and possibly contributing to the observed slow upper-mantle velocities and active volcanism in the Central Anatolian Volcanic Province above the vertical block. Additionally, detachment of the vertical block and potential rebound of the buoyant continental material have previously been interpreted to contribute to recent uplift of the Central Taurus Mountains (Schildgen et al., 2014; Abgarmi et al., 2017; Delph et al., 2017).

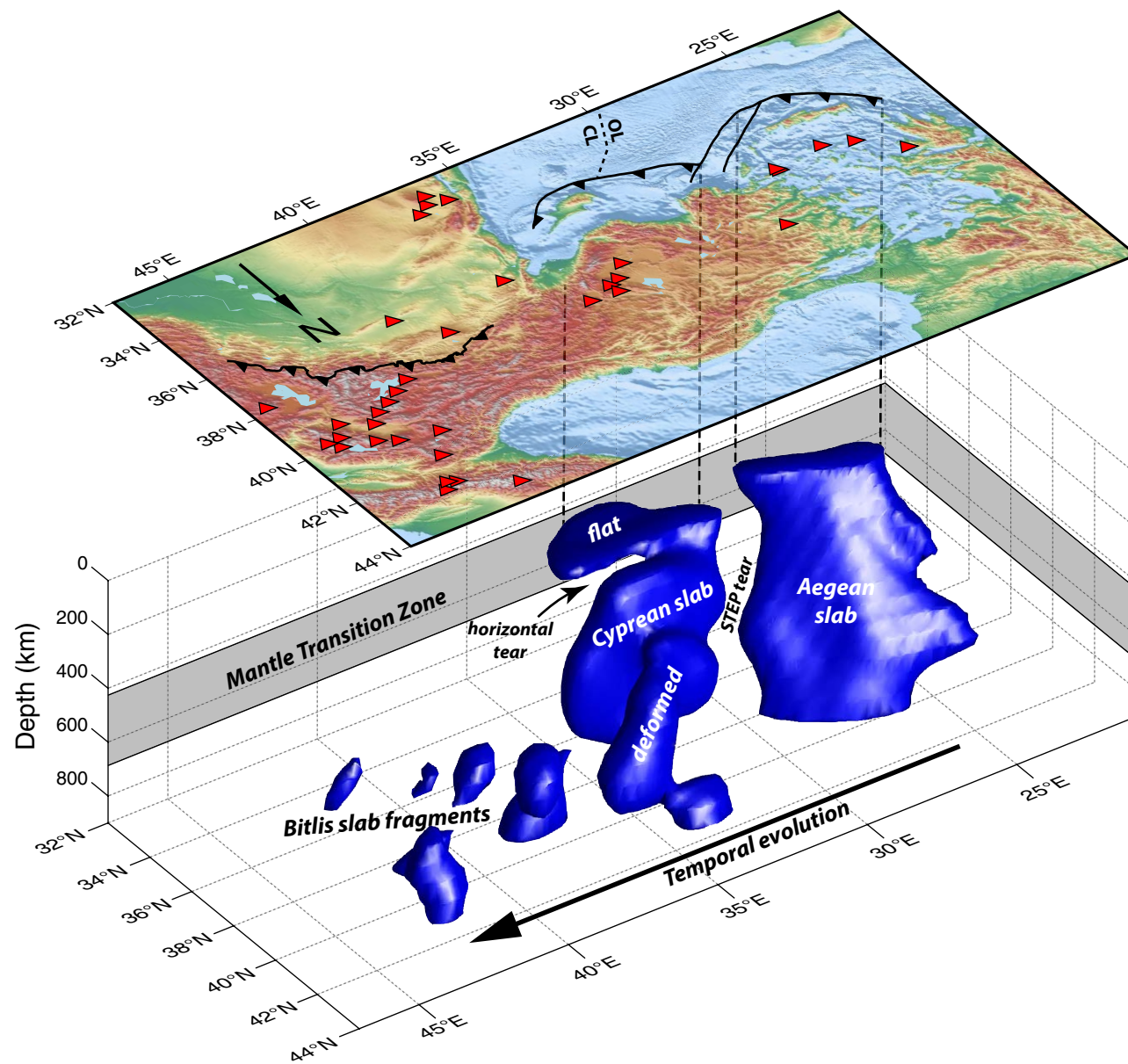


Figure 8. Diagrammatic representation of the interpreted slab geometry for each convergent domain. To create the isosurface, a synthetic velocity structure imitating our interpretation of the slab structure was created, and a synthetic recovery test was performed. The isosurface itself is an isovelocity contour of the output model of the synthetic test. As such, the surface is not derived from data and is not a quantitative representation of the tomography model, but is instead our interpretation. Red triangles indicate volcanoes active in the Holocene. OL—oceanic lithosphere; CL—continental lithosphere; STEP—subduction-transform edge propagator system.

Bitlis-Zagros Slabs

To the east of the Cyprean trench, there is the Bitlis-Zagros suture zone, which demarcates the former subduction margin of the once-expansive Neo-Tethys Ocean (Şengör and Kidd, 1979; Bozkurt, 2001; Okay et al., 2010). This segment bridges the gap between the active subduction zone at the Cyprean trench to the west and the Zagros collision front to the east. We observe the eastern edge of the Cyprean slab at longitude 35°E in our tomography model. The Zagros slab to the east has been well imaged with teleseismic tomography (Alinaghi et al., 2007), but poor resolution on the edge of that model prevented a clear demarcation of the western edge of the Zagros slab. Similarly, our model has poor resolution of the Zagros slab, but we do observe a fast velocity anomaly just outside our well-resolved model space (labeled as “Zagros slab?” in Fig. 6). This confirms that the Zagros slab fast anomaly is not continuous with the Cyprean slab anomaly across the Bitlis-Zagros suture zone. Instead, the upper mantle is dominated by slow velocity anomalies—a marked contrast to the Aegean and Cyprean domains, which each contain prominent fast velocity anomalies in the upper mantle. Since collision along the Bitlis-Zagros suture zone, the subducted Neo-Tethyan lithosphere in this region, which we refer to as the Bitlis slab, steepened and detached (Keskin, 2003; Şengör et al., 2003; Keskin, 2007) and likely sank into the mantle. Sinking of the Bitlis slab and the resultant upwelling of asthenosphere are often interpreted to be the source of slow upper-mantle velocities beneath eastern Anatolia (Lei and Zhao, 2007; Zor, 2008). Thus, our results are consistent with slab detachment beneath eastern Anatolia, but they raise the question of the current whereabouts of the detached slab.

One approach to predicting the current lateral location of the detached Bitlis slab is to assume steady plate kinematics since the time of detachment ca. 10 Ma (Şengör et al., 2003). If we assume that (1) Arabian plate velocity has been nearly constant since the early Miocene (ArRajehi et al., 2010) with absolute velocities of ~35 mm/yr WNW, (2) the slab detached at the reconstructed location of the Bitlis-Zagros suture zone, and (3) the slab sank vertically since detachment, then we predict that the detached Bitlis slab should be roughly 350 km to the ESE of the Bitlis-Zagros suture zone, in the same location as the imaged Zagros slab (Alinaghi et al., 2007). This would imply that the poorly resolved fast anomaly we see in the southeast portion of our model could be the Bitlis slab rather than the Zagros slab. However, this interpretation does not allow for the observed fast velocity anomalies to comprise the total volume of subducted lithosphere, which we would expect to span the entire margin. If the poorly resolved fast velocity anomaly is in fact the Bitlis slab, then there is no space in the mantle to accommodate the subduction of the Zagros slab to the east, suggesting the anomaly is unlikely to be the Bitlis slab. This further implies that a cohesive Bitlis slab is not present at these depths (~350 km and below), or it has migrated laterally outside of our model domain, presumably due to ambient mantle flow.

Another possible anomaly that could account for the Bitlis slab is anomaly EAF (Figs. 6A and 6B). Previous authors have interpreted this anomaly to rep-

resent the detached Bitlis slab (Lei and Zhao, 2007; Bakırcı et al., 2012). However, the observed anomaly accounts for only a small portion of the expected subducted slab volume. If it represents the detached Bitlis slab, its presence at 100 km also implies the body was dense enough to detach from the Arabian plate at the surface, but it must have quickly become neutrally buoyant, allowing it to remain at shallow depths from the mid-Miocene to the present.

Instead of these two possibilities, neither of which can account for the assumed once laterally continuous subducted slab, we consider it more likely that the Bitlis slab did not detach as a large, intact body, but rather the Bitlis slab fragmented as it detached. Around 11–10 Ma, collision and tearing of the leading oceanic lithosphere allowed for the opening of a slab window and subsequent asthenospheric upwelling (Keskin, 2003; Şengör et al., 2003). Following this initial opening, further tearing and deformation caused the subducted slab to fragment, leading to the dispersed, small, and low-amplitude fast velocity anomalies seen in our images (Fig. 7D). These anomalies, and thus the fragmented Bitlis slab, are located beneath eastern Anatolia between the Cyprean and Zagros slabs, indicating that detachment, deformation, and fragmentation are not instantaneous, but rather represent a multistage process (Wortel and Spakman, 2000; Govers and Wortel, 2005). This in turn prevents the detaching Bitlis slab from decoupling from the surrounding Cyprean and Zagros slabs and sinking independently of plate motion. The Bitlis slab fragments have not previously been imaged as seen in this study. However, analyses of conversion amplitudes from the 410 and 660 km discontinuities and transition zone thickness beneath eastern Anatolia using the receiver function technique suggest that cold temperatures influence phase conversions in this region (Ozacar et al., 2008). Ozacar et al. (2008) interpreted this as the presence of fragments of delaminated Eurasian lithosphere, rather than African-derived lithosphere. As noted in that study, however, the presence of cold slab fragments is equally consistent with the observed variations in transition zone thickness.

Given the wide range of upper-mantle slab sinking rates in the literature (Billen, 2010; van der Meer et al., 2010; Butterworth et al., 2014; Ballmer et al., 2015), it is difficult to determine if the depth of the Bitlis slab fragments matches the inferred mid-Miocene timing of slab break-off. One common way to investigate the appropriate depth is to assume that slab sinking speed is equal to convergence rate (Schellart et al., 2009). With an Arabia-Eurasia convergence rate of 15 mm/yr, this amounts to a slab depth of ~150 km after a 10 Ma detachment. However, detachment and fragmentation of the Bitlis slab make this a minimum estimate because free sinking would likely be faster than the relatively slow Arabia-Eurasia convergence rate. The high end of estimated sinking rates (up to 150 mm/yr) would place the slab well into the lower mantle and possibly below our model domain, even when considering a sinking deceleration in the lower mantle (Lithgow-Bertelloni and Richards, 1998). While this would provide an alternative explanation for the lack of a continuous fast velocity anomaly, these rates are considered outliers, as sinking rates >60 mm/yr only apply to continuous slabs that have stalled in the mantle transition zone (Billen, 2010). Thus, having the shallowest Bitlis fragments visible within

our model domain in the transition zone and uppermost lower mantle is consistent with our interpretation.

Interpreting the disparate fast velocity anomalies beneath eastern Anatolia as slab fragments requires that the small, low-amplitude fast velocity anomalies we image are robust. While it is difficult to prove that such low-amplitude anomalies are not artifacts of the tomographic inversion, we show that anomalies of that magnitude beneath eastern Anatolia are unlikely to appear without true fast velocities. This is made clear with synthetic recovery tests of slab fragments with varying input amplitude (Fig. S9 [footnote 1]). In such tests, only true velocity anomalies with high amplitude (at least 3%) yield recovered amplitudes comparable to the observed velocities. Last, synthetic tests with induced data noise (Rawlinson et al., 2014) indicate that unreasonably high amounts of noise (>100% of model misfit) are required to produce anomalies as strong as the interpreted fragments beneath eastern Anatolia (Fig. S10 [footnote 1]). These tests are described in more detail in the Supplemental Material (see footnote 1).

Slabs in the Transition Zone

One key feature of the Biryol et al. (2011) model is that each of the subducted slabs beneath Anatolia appears to flatten in the mantle transition zone, at least temporarily. However, this may be an artifact resulting from a model domain that does not extend into the lower mantle. As we find in our model, significant amplitude is artificially placed in the deepest layers of the model during inversion (Fig. S4 [footnote 1]). It is likely that a similar effect occurred during inversion for the model of Biryol et al. (2011), such that artificially fast velocity anomalies were seen to be continuous and flat-lying in the mantle transition zone.

Our new model differs from the model of Biryol et al. (2011) in that the model domain extends into the lower mantle, allowing for the assessment of the subducting African lithosphere's interactions with the 660 km discontinuity. Seismic tomography (Fukao et al., 2001; Scire et al., 2017) and geodynamic modeling (Čížková et al., 2007; Billen, 2010; Stegman et al., 2010; Garel et al., 2014) studies indicate that the viscosity jump observed at the base of the mantle transition zone (Quinteros et al., 2010; Rudolph et al., 2015) may serve to inhibit slab descent through stagnation and/or deformation. The way in which the subducting plate interacts with the mantle transition zone has broad implications for processes such as mantle convection (van der Hilst et al., 1997), overriding plate volcanism (Richard and Iwamori, 2010), and possibly for orogenic plateau development (Faccenna et al., 2013).

In the Mediterranean region, southward trench migration from slab rollback is generally thought to cause stagnation in the mantle transition zone as the 660 km discontinuity serves to block slab descent into the lower mantle (Wortel and Spakman, 2000; Piromallo and Morelli, 2003). This constrains mantle convection to the upper mantle, which may have a significant impact on surface kinematics and deformation (Faccenna et al., 2013, 2014). Previous seismic imaging efforts differ on how slabs beneath Anatolia relate to this

model. While the regional tomography model of Biryol et al. (2011) shows the subducted lithosphere lying flat in the mantle transition zone, global tomography models show that the subducted lithosphere beneath Anatolia may temporarily stagnate, but eventually sinks into the lower mantle (Bijwaard et al., 1998; Piromallo and Morelli, 2003). In our new model, fast seismic velocity perturbations do not dominate the mantle transition zone (Figs. 5, 6, and 7), appearing more disjointed, but they nonetheless continue into the lower mantle throughout the study area (Figs. 6E and 6F).

In the Aegean domain, the Aegean slab anomaly is continuous from the surface into the lower mantle, appearing to traverse the transition zone relatively uninhibited (Fig. 7A). It is possible that the thickness of the Aegean slab fast velocity anomaly in the transition zone (~300 km) indicates deformation associated with slab penetration into the lower mantle (Stegman et al., 2010; Garel et al., 2014). However, due to a number of factors, including the relatively constant thickness of the slab anomaly and continuous penetration into the lower mantle, we consider the slab thickness to more likely result from a combination of tomographic smearing in the Aegean region and the 3-D concave structure of the Aegean slab. In the Cyprean domain, the vertical limb of the Cyprean slab anomaly cohesively extends to the base of the transition zone without penetrating to the lower mantle (anomaly EC2; Fig. 7C). However, north of the vertical block, lower-amplitude fast velocity perturbations extend from the transition zone into the lower mantle (anomaly EC3). While the vertical block itself appears continuous in its descent, one interpretation is that, contrary to the Aegean slab, the vertical Cyprean slab block buckles upon interacting with the 660 km discontinuity. Weaker fast velocities in front of the separated block may be fragments of older Cyprean slab that have broken off, piled up, and eventually sunk into the lower mantle. Thus, in central Anatolia, the 660 km discontinuity induces slab deformation but allows for slab penetration to the lower mantle in lieu of stagnation. In the Bitlis-Zagros domain (Fig. 7D), disparate fast velocity bodies are scattered within the transition zone and uppermost lower mantle. We similarly interpret these fast velocity anomalies as fragments of the detached Bitlis slab, though it is unclear whether fragmentation was associated with the slab's interaction with the 660 km discontinuity or took place at shallower depths. As with the Cyprean slab, fast velocity perturbations in the uppermost lower mantle indicate that the 660 km discontinuity does not prevent the descent of the deformed Bitlis slab fragments into the lower mantle. Across each domain, contrary to the greater Mediterranean system, the viscosity boundary associated with the transition from the upper to lower mantle does not appear to cause long-term stagnation of Eastern Mediterranean slabs in the mantle transition zone, but instead likely induces at least some slab deformation.

Terminal Stages of Subduction

The traditional view of subduction is one in which denser lithosphere descends into the upper mantle, possibly stalling in the transition zone due to a viscosity contrast at the 660 km discontinuity (Fukao et al., 2001; Goes et al., 2017), before coming to rest near the core-mantle boundary (Wysession, 1996;

Rao and Kumar, 2014). However, evidence is mounting that many slabs do not follow such a simple path (Nolet, 2009). In particular, Mediterranean slabs are seen to significantly deform prior to reaching the 660 km discontinuity (von Blanckenburg and Davies, 1995; Wortel and Spakman, 2000; Biryol et al., 2011) and often do not readily continue their descent into the lower mantle (Piromallo and Morelli, 2003). Eventually, continental impingement on a trench may lead to detachment of the slab and a transition from subduction to collision, as inferred from seismic tomography in the India-Asia collision (Van der Voo et al., 1999b; Koulakov and Sobolev, 2006).

Anatolia marks a major transition from primarily oceanic subduction in the west to continental collision in the east, separated by a transitional segment in central Anatolia where attenuated continental lithosphere is subducting. In Anatolia, we suggest that we can relate the variable morphology of subducting lithosphere across three distinct convergent domains with the temporal evolution of subduction termination. Thus, Figure 8 can be viewed not only as an interpretation of the modern mantle structure beneath Anatolia, but additionally as a depiction of the temporal evolution of the subduction termination process when viewed from west to east. With this model, the Aegean domain represents the continuous subduction of oceanic lithosphere beneath a continental upper plate, which occurs throughout the majority of the lifetime of a subduction zone. In this domain, we observe a Wadati-Benioff zone down to ~200 km depth and a continuous, relatively undeformed slab extending from the surface down into the lower mantle. East of the Aegean domain, the Cyprean domain represents subduction actively transitioning to termination. Here, slab character is variable, in that the western Cyprean slab appears continuous with a consistent dip and a Wadati-Benioff zone extending to ~150 km depth, while the eastern Cyprean slab exhibits signs of severe deformation and fragmentation, with a horizontal tear separating slab segments of distinct dip. The variation in subduction character within the Cyprean domain is likely determined by the character of material entering the trench on the downgoing plate, with oceanic lithosphere subducting at the western Cyprean trench and thinned continental lithosphere further to the east (Figs. 1 and 8). The severe, shallow slab deformation associated with the impingement of continental lithosphere on the trench is evidence in the mantle that the Cyprean domain is both a spatial transition from the Aegean domain and a transition in subduction stage. Finally, the Bitlis-Zagros domain east of the Cyprean domain represents the final stage in the transition from subduction to the collision of two continental plates and the complete removal of the subducting lithosphere. Subduction is thought to have ended ca. 10 Ma in this region following collision and slab detachment (Keskin, 2003; Şengör et al., 2003), such that the most recently subducted slab has likely descended to at least the mantle transition zone. What remains is a collection of torn, deformed fragments of Bitlis slab with a weakened seismic signature. This evolutionary model predicts that the mantle character of the eastern Cyprean domain is approximately what subduction in the Bitlis-Zagros domain may have looked like ca. 10 Ma, and what the Aegean domain will look like when the African continental margin begins to enter the Aegean Trench. This model additionally has significant im-

plications for the fate of subducted material. While some slabs may be able to cohesively traverse the mantle to the core-mantle boundary (Wyssession, 1996), our images suggest that in other cases, slab destruction and assimilation are catalyzed at much shallower depths by tearing and fragmentation upon continental collision.

CONCLUSIONS

We used finite-frequency teleseismic P-wave tomography to obtain an improved seismic velocity model of the Eastern Mediterranean mantle. Our new P-wave tomography model reveals the complex, segmented structure of subducting African-Arabian lithosphere beneath Anatolia and its interactions with the surrounding mantle and the mantle transition zone in three separate convergent domains. Three main conclusions can be drawn across convergent domains:

(1) Our model confirms the work of several well-established features of Anatolian mantle velocity structure shown in prior seismic studies, including: (a) a continuous fast velocity anomaly associated with the Aegean slab extending from the surface into the lower mantle, (b) widespread slow velocities in the shallow mantle beneath Anatolia, with particularly slow velocities throughout the upper mantle beneath eastern Anatolia, and (c) fast seismic velocities in the shallow mantle north of the Izmir-Ankara-Erzincan suture zone.

(2) Slabs in the Eastern Mediterranean interact with the 660 km discontinuity differently than is generally observed in the greater Mediterranean system. Rather than flattening in the mantle transition zone, slabs beneath Anatolia all appear to descend into the lower mantle, with the Aegean slab crossing the discontinuity unimpeded, the Cyprean slab continuing into the lower mantle with signs of significant deformation in the mantle transition zone, and a significantly fragmented Bitlis slab appearing both above and below the 660 km discontinuity.

(3) The distinct character of subduction within each convergent domain is correlated with the material entering the trench on the downgoing plate, varying from oceanic lithosphere subducting at the Aegean Trench to continental lithosphere colliding with eastern Anatolia at the Bitlis-Zagros suture zone. This allows us to interpret spatial variations in slab structure as different temporal stages of subduction termination. The Aegean slab is undergoing little to no deformation as it dips continuously into the lower mantle, implying it is in its main subduction stage. The Cyprean slab, which is severely deformed through tearing and fragmentation, is the middle stage between those of the Aegean and Bitlis slabs, when continental lithosphere is beginning to underthrust at the trench, likely blocking subduction, inducing tearing, and initiating the breakup of the downgoing Cyprean slab. Thus, the Cyprean slab exhibits subduction termination in progress. The Bitlis slab is completely fragmented within and below the mantle transition zone and shows no continuity with the surface plate, indicating a complete transition from subduction to continental collision in the Bitlis-Zagros domain. This model has significant implications

for our view of a slab's life cycle, suggesting that some slabs may significantly fragment at the end of subduction rather than cohesively sink through the mantle after detachment.

ACKNOWLEDGMENTS

We would like to thank the extraordinary efforts made by the entire Continental Dynamics–Central Anatolian Tectonics (CD-CAT) team, both in collecting our critical seismic data set and in invaluable workshops that have made this article possible. We would also like to thank Brandon Schmandt and Alissa Scire for thoughtful consultations on the finite-frequency tomography method. Last, we would like to thank two anonymous reviewers for thorough, thoughtful revisions that helped to greatly improve this manuscript. This research was supported by National Science Foundation grant EAR-1109336 (CD-CAT). Delph was supported by the Wiess Postdoctoral Research Fellowship at Rice University. The tomography model from this study will be made available online through the IRIS Earth Model Collaboration (<http://ds.iris.edu/ds/products/emc/>) with the label ANA2_P_2018.

REFERENCES CITED

- Abgarmi, B., Delph, J.R., Ozacar, A.A., Beck, S.L., Zandt, G., Sandvol, E., Turkelli, N., and Biryol, C.B., 2017, Structure of the crust and African slab beneath the Central Anatolian Plateau from receiver functions: New insights on isostatic compensation and slab dynamics: *Geosphere*, v. 13, p. 1774–1787, <https://doi.org/10.1130/GES01509.1>.
- Albuquerque Seismological Laboratory (ASL)/U.S. Geological Survey (USGS), 1988, Global Seismograph Network (GSN-IRIS/USGS), <https://doi.org/10.7914/SN/IU>.
- Alinaghi, A., Koulakov, I., and Thybo, H., 2007, Seismic tomographic imaging of P- and S-wave velocity perturbations in the upper mantle beneath Iran: *Geophysical Journal International*, v. 169, p. 1089–1102, <https://doi.org/10.1111/j.1365-246X.2007.03317.x>.
- Angus, D.A., Wilson, D.C., Sandvol, E., and Ni, J.F., 2006, Lithospheric structure of the Arabian and Eurasian collision zone in eastern Turkey from S-wave receiver functions: *Geophysical Journal International*, v. 166, p. 1335–1346, <https://doi.org/10.1111/j.1365-246X.2006.03070.x>.
- ArRajehi, A., McClusky, S., Reilinger, R., Daoud, M., Alchalbi, A., Ergintav, S., Gomez, F., Sholan, J., Bou-Rabee, F., Ogubazghi, G., Haileab, B., Fisseha, S., Asfaw, L., Mahmoud, S., et al., 2010, Geodetic constraints on present-day motion of the Arabian plate: Implications for Red Sea and Gulf of Aden rifting: *Tectonics*, v. 29, TC3011, <https://doi.org/10.1029/2009TC002482>.
- Bakırcı, T., Yoshizawa, K., and Özer, M.F., 2012, Three-dimensional S-wave structure of the upper mantle beneath Turkey from surface wave tomography: *Geophysical Journal International*, v. 190, p. 1058–1076, <https://doi.org/10.1111/j.1365-246X.2012.05526.x>.
- Ballmer, M.D., Schmerr, N.C., Nakagawa, T., and Ritsema, J., 2015, Compositional mantle layering revealed by slab stagnation at 1000-km depth: *Science Advances*, v. 1, p. e1500815, <https://doi.org/10.1126/sciadv.1500815>.
- Barka, A., and Reilinger, R., 1997, Active tectonics of the Eastern Mediterranean region: Deduced from GPS, neotectonic and seismic data: *Annali di Geofisica*, v. XL, p. 587–610.
- Bartol, J., and Govers, R., 2014, A single cause for uplift of the Central and Eastern Anatolian Plateau?: *Tectonophysics*, v. 637, p. 116–136, <https://doi.org/10.1016/j.tecto.2014.10.002>.
- Beck, S., and Zandt, G., 2005, Continental lithospheric deformation along a major strike-slip fault zone: The central North Anatolian fault zone, Turkey: *International Federation of Digital Seismograph Networks*, https://doi.org/10.7914/SN/YL_2005.
- Bijwaard, H., Spakman, W., and Engdahl, E.R., 1998, Closing the gap between regional and global travel time tomography: *Journal of Geophysical Research*, v. 103, p. 30,055–30,078, <https://doi.org/10.1029/98JB02467>.
- Billen, M.I., 2010, Slab dynamics in the transition zone: *Physics of the Earth and Planetary Interiors*, v. 183, p. 296–308, <https://doi.org/10.1016/j.pepi.2010.05.005>.
- Biryol, C.B., Beck, S.L., Zandt, G., and Özacar, A.A., 2011, Segmented African lithosphere beneath the Anatolian region inferred from teleseismic P-wave tomography: *Geophysical Journal International*, v. 184, p. 1037–1057, <https://doi.org/10.1111/j.1365-246X.2010.04910.x>.
- Bogazici University Kandilli Observatory and Earthquake Research Institute, 2001, Bogazici University Kandilli Observatory and Earthquake Research Institute, <https://doi.org/10.7914/SN/KO>.
- Bozkurt, E., 2001, Neotectonics of Turkey—A synthesis: *Geodinamica Acta*, v. 14, p. 3–30, <https://doi.org/10.1080/09853111.2001.11432432>.
- Butterworth, N.P., Talsma, A.S., Müller, R.D., Seton, M., Bunge, H.-P., Schubert, B.S.A., Shephard, G.E., and Heine, C., 2014, Geological, tomographic, kinematic and geodynamic constraints on the dynamics of sinking slabs: *Journal of Geodynamics*, v. 73, p. 1–13, <https://doi.org/10.1016/j.jog.2013.10.006>.
- Čížková, H., van Hunen, J., and van den Berg, A., 2007, Stress distribution within subducting slabs and their deformation in the transition zone: *Physics of the Earth and Planetary Interiors*, v. 161, p. 202–214, <https://doi.org/10.1016/j.pepi.2007.02.002>.
- Cosentino, D., Schildgen, T.F., Cipollari, P., Faranda, C., Gliozzi, E., Hudackova, N., Lucifora, S., and Strecker, M.R., 2012, Late Miocene surface uplift of the southern margin of the Central Anatolian Plateau, Central Taurides, Turkey: *Geological Society of America Bulletin*, v. 124, p. 133–145, <https://doi.org/10.1130/B30466.1>.
- Dahlen, F.A., Hung, S.-H., and Nolet, G., 2000, Frechet kernels for finite-frequency traveltimes: I. Theory: *Geophysical Journal International*, v. 141, p. 157–174, <https://doi.org/10.1046/j.1365-246X.2000.00070.x>.
- de Boorder, H., Spakman, W., White, S.H., and Wortel, M.J.R., 1998, Late Cenozoic mineralization, orogenic collapse and slab detachment in the European Alpine Belt: *Earth and Planetary Science Letters*, v. 164, p. 569–575, [https://doi.org/10.1016/S0012-821X\(98\)00247-7](https://doi.org/10.1016/S0012-821X(98)00247-7).
- Delph, J.R., Biryol, C.B., Beck, S.L., Zandt, G., and Ward, K.M., 2015a, Shear wave velocity structure of the Anatolian plate: Anomalously slow crust in southwestern Turkey: *Geophysical Journal International*, v. 202, p. 261–276, <https://doi.org/10.1093/gji/ggv141>.
- Delph, J.R., Zandt, G., and Beck, S.L., 2015b, A new approach to obtaining a 3D shear wave velocity model of the crust and upper mantle: An application to eastern Turkey: *Tectonophysics*, v. 665, p. 92–100, <https://doi.org/10.1016/j.tecto.2015.09.031>.
- Delph, J.R., Abgarmi, B., Ward, K.M., Beck, S.L., Özacar, A.A., Zandt, G., Sandvol, E., Türkelli, N., and Kalafat, D., 2017, The effects of subduction termination on the continental lithosphere: Linking volcanism, deformation, surface uplift, and slab tearing in central Anatolia: *Geosphere*, v. 13, p. 1788–1805, <https://doi.org/10.1130/GES01478.1>.
- Dilek, Y., and Altunkaynak, Ş., 2009, Geochemical and temporal evolution of Cenozoic magmatism in western Turkey: Mantle response to collision, slab break-off, and lithospheric tearing in an orogenic belt, *in* van Hinsbergen, D.J.J., Edwards, M.A., and Govers, R., eds., *Collision and Collapse at the Africa-Arabia-Eurasia Subduction Zone*: Geological Society, London, Special Publication 311, p. 213–233, <https://doi.org/10.1144/SP311.8>.
- Domeier, M., Doubrovine, P.V., Torsvik, T.H., Spakman, W., and Bull, A.L., 2016, Global correlation of lower mantle structure and past subduction: *Geophysical Research Letters*, v. 43, p. 4945–4953, <https://doi.org/10.1002/2016GL068827>.
- Duret, T., Gerya, T.V., and Spakman, W., 2014, Slab detachment in laterally varying subduction zones: 3-D numerical modeling: *Geophysical Research Letters*, v. 41, p. 1951–1956, <https://doi.org/10.1002/2014GL059472>.
- Espurt, N., Hippolyte, J.-C., Kaymakci, N., and Sangu, E., 2014, Lithospheric structural control on inversion of the southern margin of the Black Sea Basin, Central Pontides, Turkey: *Lithosphere*, v. 6, p. 26–34, <https://doi.org/10.1130/L316.1>.
- Faccenna, C., and Becker, T.W., 2010, Shaping mobile belts by small-scale convection: *Nature*, v. 465, p. 602–605, <https://doi.org/10.1038/nature09064>.
- Faccenna, C., Jolivet, L., Piromallo, C., and Morelli, A., 2003, Subduction and the depth of convection in the Mediterranean mantle: *Journal of Geophysical Research—Solid Earth*, v. 108, 2099, <https://doi.org/10.1029/2001JB001690>.
- Faccenna, C., Becker, T.W., Conrad, C.P., and Husson, L., 2013, Mountain building and mantle dynamics: *Tectonics*, v. 32, p. 80–93, <https://doi.org/10.1029/2012TC003176>.
- Faccenna, C., Becker, T.W., Auer, L., Billi, A., Boschi, L., Brun, J.P., Capitanio, F.A., Funicello, F., Horváth, F., Jolivet, L., Piromallo, C., Royden, L., Rossetti, F., and Serpelloni, E., 2014, Mantle dynamics in the Mediterranean: *Reviews of Geophysics*, v. 52, p. 283–332, <https://doi.org/10.1002/2013RG000444>.
- Fayon, A.K., and Whitney, D.L., 2007, Interpretation of tectonic versus magmatic processes for resetting apatite fission track ages in the Niğde Massif, Turkey: *Tectonophysics*, v. 434, p. 1–13, <https://doi.org/10.1016/j.tecto.2007.01.003>.
- Fichtner, A., Saygin, E., Taymaz, T., Cupillard, P., Capdeville, Y., and Trampert, J., 2013, The deep structure of the North Anatolian fault zone: *Earth and Planetary Science Letters*, v. 373, p. 109–117, <https://doi.org/10.1016/j.epsl.2013.04.027>.

- Francalanci, L., Innocenti, F., Manetti, P., and Savascin, M.Y., 2000, Neogene alkaline volcanism of the Afyon-Isparta area, Turkey: Petrogenesis and geodynamic implications: *Mineralogy and Petrology*, v. 70, p. 285–312, <https://doi.org/10.1007/s007100070007>.
- Fukao, Y., Widiyantoro, S., and Obayashi, M., 2001, Stagnant slabs in the upper and lower mantle transition region: *Reviews of Geophysics*, v. 39, p. 291–323, <https://doi.org/10.1029/1999RG000068>.
- Gans, C.R., Beck, S.L., Zandt, G., Biryol, C.B., and Özacar, A.A., 2009, Detecting the limit of slab break-off in central Turkey: New high-resolution Pn tomography results: *Geophysical Journal International*, v. 179, p. 1566–1572, <https://doi.org/10.1111/j.1365-246X.2009.04389.x>.
- Garel, F., Goes, S., Davies, D.R., Davies, J.H., Kramer, S.C., and Wilson, C.R., 2014, Interaction of subducted slabs with the mantle transition-zone: A regime diagram from 2-D thermo-mechanical models with a mobile trench and an overriding plate: *Geochemistry Geophysics Geosystems*, v. 15, p. 1739–1765, <https://doi.org/10.1002/2014GC005257>.
- GEOFON Data Centre, 1993, GEOFON Seismic Network: <https://doi.org/10.14470/TR560404>.
- Goes, S., Agrusta, R., van Hunen, J., and Garel, F., 2017, Subduction-transition zone interaction: A review: *Geosphere*, v. 13, no. 3, p. 644–664, <https://doi.org/10.1130/GES01476.1>.
- Göğüş, O.H., and Psyklywec, R.N., 2008, Mantle lithosphere delamination driving plateau uplift and synconvergent extension in eastern Anatolia: *Geology*, v. 36, p. 723–726, <https://doi.org/10.1130/G24982A.1>.
- Göğüş, O.H., Psyklywec, R.N., Şengör, A.M.C., and Gün, E., 2017, Drip tectonics and the enigmatic uplift of the Central Anatolian Plateau: *Nature Communications*, v. 8, p. 1538, <https://doi.org/10.1038/s41467-017-01611-3>.
- Gök, R., Pasyanos, M.E., and Zor, E., 2007, Lithospheric structure of the continent-continent collision zone: Eastern Turkey: *Geophysical Journal International*, v. 169, p. 1079–1088, <https://doi.org/10.1111/j.1365-246X.2006.03288.x>.
- Govers, R., and Fichtner, A., 2016, Signature of slab fragmentation beneath Anatolia from full-waveform tomography: *Earth and Planetary Science Letters*, v. 450, p. 10–19, <https://doi.org/10.1016/j.epsl.2016.06.014>.
- Govers, R., and Wortel, M.J.R., 2005, Lithosphere tearing at STEP faults: Response to edges of subduction zones: *Earth and Planetary Science Letters*, v. 236, p. 505–523, <https://doi.org/10.1016/j.epsl.2005.03.022>.
- Granot, R., 2016, Palaeozoic oceanic crust preserved beneath the Eastern Mediterranean: *Nature Geoscience*, v. 9, p. 701–705, <https://doi.org/10.1038/ngeo2784>.
- Gürer, D., van Hinsbergen, D.J.J., Matenco, L., Corfu, F., and Casella, A., 2016, Kinematics of a former oceanic plate of the Neotethys revealed by deformation in the Ulukışla basin (Turkey): *Tectonics*, v. 35, p. 2385–2416, <https://doi.org/10.1002/2016TC004206>.
- Hafkenscheid, E., Wortel, M.J.R., and Spakman, W., 2006, Subduction history of the Tethyan region derived from seismic tomography and tectonic reconstructions: *Journal of Geophysical Research—Solid Earth*, v. 111, B08401, <https://doi.org/10.1029/2005JB003791>.
- Higgins, M., Schoenbohm, L.M., Brocard, G., Kaymakci, N., Gosse, J.C., and Cosca, M.A., 2015, New kinematic and geochronologic evidence for the Quaternary evolution of the Central Anatolian fault zone (CAFZ): *Tectonics*, v. 34, p. 2118–2141, <https://doi.org/10.1002/2015TC003864>.
- Jiménez-Munt, I., Sabadini, R., Gardi, A., and Bianco, G., 2003, Active deformation in the Mediterranean from Gibraltar to Anatolia inferred from numerical modeling and geodetic and seismological data: *Journal of Geophysical Research—Solid Earth*, v. 108, p. ETG 2-1–ETG 2-24, <https://doi.org/10.1029/2001JB001544>.
- Jolivet, L., Faccenna, C., Huet, B., Labrousse, L., Le Pourhiet, L., Lacombe, O., Lecomte, E., Burrov, E., Denèle, Y., Brun, J.P., Philippon, M., Paul, A., Salaün, G., Karabulut, H., et al., 2013, Aegean tectonics: Strain localisation, slab tearing and trench retreat: *Tectonophysics*, v. 597–598, p. 1–33, <https://doi.org/10.1016/j.tecto.2012.06.011>.
- Karabulut, H., Paul, A., Afacan Ergün, T., Hatzfeld, D., Childs, D.M., and Aktar, M., 2013, Long-wavelength undulations of the seismic Moho beneath the strongly stretched western Anatolia: *Geophysical Journal International*, v. 194, p. 450–464, <https://doi.org/10.1093/gji/ggt100>.
- Kennett, B.L.N., and Engdahl, E.R., 1991, Traveltimes for global earthquake location and phase identification: *Geophysical Journal International*, v. 105, p. 429–465, <https://doi.org/10.1111/j.1365-246X.1991.tb06724.x>.
- Keskin, M., 2003, Magma generation by slab steepening and breakoff beneath a subduction-accretion complex: An alternative model for collision-related volcanism in eastern Anatolia, Turkey: *Geophysical Research Letters*, v. 30, p. 7–10, <https://doi.org/10.1029/2003GL018019>.
- Keskin, M., 2007, Eastern Anatolia: A hotspot in a collision zone without a mantle plume, *in* Foulger, G.R., and Jurdy, D.M., eds., *Plates, Plumes, and Planetary Processes: Geological Society of America Special Paper 430*, p. 693–722, [https://doi.org/10.1130/2007.2430\(32\)](https://doi.org/10.1130/2007.2430(32)).
- Koçyiğit, A., and Beyhan, A., 1998, A new intracontinental transcurent structure: The Central Anatolian fault zone, Turkey: *Tectonophysics*, v. 284, p. 317–336, [https://doi.org/10.1016/S0040-1951\(97\)00176-5](https://doi.org/10.1016/S0040-1951(97)00176-5).
- Koulakov, I., and Sobolev, S.V., 2006, A tomographic image of Indian lithosphere break-off beneath the Pamir-Hindukush region: *Geophysical Journal International*, v. 164, p. 425–440, <https://doi.org/10.1111/j.1365-246X.2005.02841.x>.
- Kuscu, G.G., and Genel, F., 2010, Review of post-collisional volcanism in the Central Anatolian Volcanic Province (Turkey), with special reference to the Tepeky volcanic complex: *International Journal of Earth Sciences*, v. 99, p. 593–621, <https://doi.org/10.1007/s00531-008-0402-4>.
- Lei, J., and Zhao, D., 2007, Teleseismic evidence for a break-off subducting slab under eastern Turkey: *Earth and Planetary Science Letters*, v. 257, p. 14–28, <https://doi.org/10.1016/j.epsl.2007.02.011>.
- Le Pichon, X., and Angelier, J., 1979, The Hellenic arc and trench system: A key to the evolution of the Eastern Mediterranean area: *Tectonophysics*, v. 60, p. 1–42, [https://doi.org/10.1016/0040-1951\(79\)90131-8](https://doi.org/10.1016/0040-1951(79)90131-8).
- Lithgow-Bertelloni, C., and Richards, M.A., 1998, The dynamics of Cenozoic and Mesozoic plate motions: *Reviews of Geophysics*, v. 36, p. 27–78, <https://doi.org/10.1029/97RG02282>.
- McKenzie, D., 1978, Active tectonics of the Alpine-Himalayan belt: The Aegean Sea and surrounding regions: *Geophysical Journal International*, v. 55, p. 217–254, <https://doi.org/10.1111/j.1365-246X.1978.tb04759.x>.
- Menant, A., Jolivet, L., and Vrielynck, B., 2016, Kinematic reconstructions and magmatic evolution illuminating crustal and mantle dynamics of the Eastern Mediterranean region since the Late Cretaceous: *Tectonophysics*, v. 675, p. 103–140, <https://doi.org/10.1016/j.tecto.2016.03.007>.
- Mitchell, B., and Zhu, L., 2002, Integrated seismological studies of crust and upper mantle structure in western Anatolia: *Geophysical Research Letters*, v. 30, https://doi.org/10.7914/SN/XH_2002.
- Mutlu, A.K., and Karabulut, H., 2011, Anisotropic Pn tomography of Turkey and adjacent regions: *Geophysical Journal International*, v. 187, p. 1743–1758, <https://doi.org/10.1111/j.1365-246X.2011.05235.x>.
- Nolet, G., 2009, Slabs do not go gently: *Science*, v. 324, p. 1152–1153, <https://doi.org/10.1126/science.1174664>.
- Nouri, F., Azizi, H., Golonka, J., Asahara, Y., Orihashi, Y., Yamamoto, K., Tsuboi, M., and Anma, R., 2016, Age and petrogenesis of Na-rich felsic rocks in western Iran: Evidence for closure of the southern branch of the Neo-Tethys in the Late Cretaceous: *Tectonophysics*, v. 671, p. 151–172, <https://doi.org/10.1016/j.tecto.2015.12.014>.
- Okay, A.I., Zattin, M., and Cavazza, W., 2010, Apatite fission-track data for the Miocene Arabia-Eurasia collision: *Geology*, v. 38, p. 35–38, <https://doi.org/10.1130/G30234.1>.
- Ozacar, A.A., Gilbert, H., and Zandt, G., 2008, Upper mantle discontinuity structure beneath East Anatolian Plateau (Turkey) from receiver functions: *Earth and Planetary Science Letters*, v. 269, p. 427–435, <https://doi.org/10.1016/j.epsl.2008.02.036>.
- Özacar, A.A., Zandt, G., Gilbert, H., and Beck, S.L., 2010, Seismic images of crustal variations beneath the East Anatolian Plateau (Turkey) from teleseismic receiver functions, *in* Sosson, M., Kaymakci, N., Stephenson, R.A., Bergerat, F., and Starostenko, V., eds., *Sedimentary Basin Tectonics from the Black Sea and Caucasus to the Arabian Platform*: Geological Society, London, Special Publication 340, p. 485–496, <https://doi.org/10.1144/SP340.21>.
- Papazachos, B.C., Karakostas, V.G., Papazachos, C.B., and Scordilis, E.M., 2000, The geometry of the Wadati-Benioff zone and lithospheric kinematics in the Hellenic arc: *Tectonophysics*, v. 319, p. 275–300, [https://doi.org/10.1016/S0040-1951\(99\)00299-1](https://doi.org/10.1016/S0040-1951(99)00299-1).
- Pavlis, G.L., and Vernon, F.L., 2010, Array processing of teleseismic body waves with the USArray: *Computers & Geosciences*, v. 36, p. 910–920, <https://doi.org/10.1016/j.cageo.2009.10.008>.
- Pearce, J.A., Bender, J.F., De Long, S.E., Kidd, W.S.F., Low, P.J., Güner, Y., Saroglu, F., Yilmaz, Y., Moorbath, S., and Mitchell, J.G., 1990, Genesis of collision volcanism in eastern Anatolia, Turkey: *Journal of Volcanology and Geothermal Research*, v. 44, p. 189–229, [https://doi.org/10.1016/0377-0273\(90\)90018-B](https://doi.org/10.1016/0377-0273(90)90018-B).
- Piromallo, C., and Morelli, A., 2003, P wave tomography of the mantle under the Alpine-Mediterranean area: *Journal of Geophysical Research*, v. 108, 2065, <https://doi.org/10.1029/2002JB001757>.

- Pourteau, A., Candan, O., and Oberhnsli, R., 2010, High-pressure metasediments in central Turkey: Constraints on the Neotethyan closure history: *Tectonics*, v. 29, TC5004, <https://doi.org/10.1029/2009TC002650>.
- Quinteros, J., Sobolev, S.V., and Popov, A.A., 2010, Viscosity in transition zone and lower mantle: Implications for slab penetration: *Geophysical Research Letters*, v. 37, L09307, <https://doi.org/10.1029/2010GL043140>.
- Rao, B.P., and Kumar, M.R., 2014, Seismic evidence for slab graveyards atop the core mantle boundary beneath the Indian Ocean geoid low: *Physics of the Earth and Planetary Interiors*, v. 236, p. 52–59, <https://doi.org/10.1016/j.pepi.2014.08.005>.
- Rawlinson, N., Fichtner, A., Sambridge, M., and Young, M.K., 2014, Seismic tomography and the assessment of uncertainty, in *Dmowska, R., ed., Advances in Geophysics*, Volume 55: Elsevier, p. 1–76, <https://doi.org/10.1016/bs.agph.2014.08.001>.
- Reid, M.R., Schleiffarth, W.K., Cosca, M.A., Delph, J.R., Blichert-Toft, J., and Cooper, K.M., 2017, Shallow melting of MORB-like mantle under hot continental lithosphere, central Anatolia: *Geochemistry Geophysics Geosystems*, v. 18, p. 1866–1888, <https://doi.org/10.1002/2016GC006772>.
- Reilinger, R., McClusky, S., Vernant, P., Lawrence, S., Ergintav, S., Cakmak, R., Ozener, H., Kadirov, F., Guliev, I., Stepanyan, R., Nadariya, M., Hahubia, G., Mahmoud, S., Sakr, K., et al., 2006, GPS constraints on continental deformation in the Africa-Arabia-Eurasia continental collision zone and implications for the dynamics of plate interactions: *Journal of Geophysical Research—Solid Earth*, v. 111, B05411, <https://doi.org/10.1029/2005JB004051>.
- Richard, G.C., and Iwamori, H., 2010, Stagnant slab, wet plumes and Cenozoic volcanism in East Asia: *Physics of the Earth and Planetary Interiors*, v. 183, p. 280–287, <https://doi.org/10.1016/j.pepi.2010.02.009>.
- Richardson-Bunbury, J.M., 1996, The Kula volcanic field, western Turkey: The development of a Holocene alkali basalt province and the adjacent normal-faulting graben: *Geological Magazine*, v. 133, p. 275–283, <https://doi.org/10.1017/S0016756800009018>.
- Robertson, A.H.F., 1998, Tectonic significance of the Eratosthenes Seamount: A continental fragment in the process of collision with a subduction zone in the Eastern Mediterranean (Ocean Drilling Program Leg 160): *Tectonophysics*, v. 298, p. 63–82, [https://doi.org/10.1016/S0040-1951\(98\)00178-4](https://doi.org/10.1016/S0040-1951(98)00178-4).
- Rudolph, M.L., Lekić, V., and Lithgow-Bertelloni, C., 2015, Viscosity jump in Earth's mid-mantle: *Science*, v. 350, p. 1349–1352, <https://doi.org/10.1126/science.1261929>.
- Salah, M.K., 2017, Lithospheric structure of southeast Anatolia from joint inversion of local and teleseismic data: *Studia Geophysica et Geodaetica*, v. 61, no. 4, p. 703–727, <https://doi.org/10.1007/s11200-016-1240-7>.
- Salaün, G., Pedersen, H.A., Paul, A., Farra, V., Karabulut, H., Hatzfeld, D., Papazachos, C., Childs, D.M., and Pequegnat, C., 2012, High-resolution surface wave tomography beneath the Aegean-Anatolia region: Constraints on upper-mantle structure: *Geophysical Journal International*, v. 190, p. 406–420, <https://doi.org/10.1111/j.1365-246X.2012.05483.x>.
- Sandvol, E., 1999, Eastern Turkey Seismic Experiment: Lithospheric Structure in an Active Continental Collision Zone: https://doi.org/10.7914/SN/XG_1999.
- Sandvol, E., 2013, Continental Dynamics/Central Anatolian Tectonics: Surface to Mantle Dynamics during Collision to Escape: https://doi.org/10.7914/SN/YB_2013.
- Savaşçın, M.Y., and Oyman, T., 1998, Tectono-magmatic evolution of alkaline volcanics at the Kirka-Afyon-Isparta trend, SW Turkey: *Turkish Journal of Earth Sciences*, v. 7, p. 201–214.
- Schattner, U., 2010, What triggered the early-to-mid Pleistocene tectonic transition across the entire Eastern Mediterranean?: *Earth and Planetary Science Letters*, v. 289, p. 539–548, <https://doi.org/10.1016/j.epsl.2009.11.048>.
- Schellart, W.P., Kennett, B.L.N., Spakman, W., and Amaru, M., 2009, Plate reconstructions and tomography reveal a fossil lower mantle slab below the Tasman Sea: *Earth and Planetary Science Letters*, v. 278, p. 143–151, <https://doi.org/10.1016/j.epsl.2008.11.004>.
- Schildgen, T.F., Cosentino, D., Bookhagen, B., Niedermann, S., Yildirim, C., Echter, H., Wittmann, H., and Strecker, M.R., 2012, Multi-phased uplift of the southern margin of the Central Anatolian Plateau, Turkey: A record of tectonic and upper mantle processes: *Earth and Planetary Science Letters*, v. 317–318, p. 85–95, <https://doi.org/10.1016/j.epsl.2011.12.003>.
- Schildgen, T.F., Yildirim, C., Cosentino, D., and Strecker, M.R., 2014, Linking slab break-off, Hellenic trench retreat, and uplift of the Central and Eastern Anatolian Plateaus: *Earth-Science Reviews*, v. 128, p. 147–168, <https://doi.org/10.1016/j.earscirev.2013.11.006>.
- Schmandt, B., and Humphreys, E., 2010, Seismic heterogeneity and small-scale convection in the southern California upper mantle: *Geochemistry Geophysics Geosystems*, v. 11, Q05004, <https://doi.org/10.1029/2010GC003042>.
- Scire, A., Zandt, G., Beck, S., Long, M., and Wagner, L., 2017, The deforming Nazca slab in the mantle transition zone and lower mantle: Constraints from teleseismic tomography on the deeply subducted slab between 6°S and 32°S: *Geosphere*, v. 13, no. 3, p. 665–680, <https://doi.org/10.1130/GES01436.1>.
- Şengör, A.M.C., and Kidd, W.S.F., 1979, Post-collisional tectonics of the Turkish-Iranian plateau and a comparison with Tibet: *Tectonophysics*, v. 55, p. 361–376, [https://doi.org/10.1016/0040-1951\(79\)90184-7](https://doi.org/10.1016/0040-1951(79)90184-7).
- Şengör, A.M.C., and Yılmaz, Y., 1981, Tethyan evolution of Turkey: A plate tectonic approach: *Tectonophysics*, v. 75, p. 181–241, [https://doi.org/10.1016/0040-1951\(81\)90275-4](https://doi.org/10.1016/0040-1951(81)90275-4).
- Şengör, A.M.C., Görür, N., and Şaroğlu, F., 1985, Strike-slip faulting and related basin formation in zones of tectonic escape: Turkey as a case study, in Biddle, K., and Christie-Blick, N., eds., *Strike-Slip Deformation, Basin Formation and Sedimentation*: Society of Economic Paleontologists and Mineralogists Special Publication 37, p. 227–264.
- Şengör, A.M.C., Özeren, S., Genç, T., and Zor, E., 2003, East Anatolian high plateau as a mantle-supported, north-south shortened domal structure: *Geophysical Research Letters*, v. 30, 8045, <https://doi.org/10.1029/2003GL017858>.
- Şengör, A.M.C., Tüysüz, O., Imren, C., Sakaç, M., Eyidoğan, H., Görür, N., Le Pichon, X., and Rangin, C., 2005, The North Anatolian fault: A new look: *Annual Review of Earth and Planetary Sciences*, v. 33, p. 37–112, <https://doi.org/10.1146/annurev.earth.32.101802.120415>.
- Şengör, A.M.C., Özeren, M.S., Keskin, M., Sakaç, M., Özbakır, A.D., and Kayan, İ., 2008, Eastern Turkish high plateau as a small Turkic-type orogen: Implications for post-collisional crust-forming processes in Turkic-type orogens: *Earth-Science Reviews*, v. 90, p. 1–48, <https://doi.org/10.1016/j.earscirev.2008.05.002>.
- Seyitoğlu, G., and Scott, B.C., 1996, The cause of N-S extensional tectonics in western Turkey: Tectonic escape vs. back-arc spreading vs. orogenic collapse: *Journal of Geodynamics*, v. 22, p. 145–153, [https://doi.org/10.1016/0264-3707\(96\)00004-X](https://doi.org/10.1016/0264-3707(96)00004-X).
- Sigloch, K., McQuarrie, N., and Nolet, G., 2008, Two-stage subduction history under North America inferred from multiple-frequency tomography: *Nature Geoscience*, v. 1, p. 458–462, <https://doi.org/10.1038/ngeo231>.
- Stegman, D.R., Farrington, R., Capitanio, F.A., and Schellart, W.P., 2010, A regime diagram for subduction styles from 3-D numerical models of free subduction: *Tectonophysics*, v. 483, p. 29–45, <https://doi.org/10.1016/j.tecto.2009.08.041>.
- Tokçaer, M., Agostini, S., and Savaşçın, M.Y., 2005, Geotectonic setting and origin of the youngest Kula volcanics (western Anatolia), with a new emplacement model: *Turkish Journal of Earth Sciences*, v. 14, p. 145–166.
- Toprak, V., 1998, Vent distribution and its relation to regional tectonics, Cappadocian volcanics, Turkey: *Journal of Volcanology and Geothermal Research*, v. 85, p. 55–67, [https://doi.org/10.1016/S0377-0273\(98\)00049-3](https://doi.org/10.1016/S0377-0273(98)00049-3).
- Toprak, V., and Göncüoğlu, M.C., 1993, Tectonic control on the development of the Neogene-Quaternary Central Anatolian Volcanic Province, Turkey: *Geological Journal*, v. 28, p. 357–369, <https://doi.org/10.1002/gj.3350280314>.
- VanDecar, J.C., and Crosson, R.S., 1990, Determination of teleseismic relative phase arrival times using multi-channel cross-correlation and least squares: *Bulletin of the Seismological Society of America*, v. 80, p. 150–169 <http://www.bssaonline.org/content/80/1/150.short>.
- van der Hilst, R.D., Widiyantoro, S., and Engdahl, E.R., 1997, Evidence for deep mantle circulation from global tomography: *Nature*, v. 386, p. 578–584, <https://doi.org/10.1038/386578a0>.
- van der Meer, D.G., Spakman, W., van Hinsbergen, D.J.J., Amaru, M.L., and Torsvik, T.H., 2010, Towards absolute plate motions constrained by lower-mantle slab remnants: *Nature Geoscience*, v. 3, p. 36–40, <https://doi.org/10.1038/ngeo708>.
- Van der Voo, R., Spakman, W., and Bijwaard, H., 1999a, Mesozoic subducted slabs under Siberia: *Nature*, v. 397, p. 246–249, <https://doi.org/10.1038/16686>.
- Van der Voo, R., Spakman, W., and Bijwaard, H., 1999b, Tethyan slabs under India: *Earth and Planetary Science Letters*, v. 171, p. 7–20, [https://doi.org/10.1016/S0012-821X\(99\)00131-4](https://doi.org/10.1016/S0012-821X(99)00131-4).
- van Hinsbergen, D.J.J., Kaymakci, N., Spakman, W., and Torsvik, T.H., 2010, Reconciling the geological history of western Turkey with plate circuits and mantle tomography: *Earth and Planetary Science Letters*, v. 297, p. 674–686, <https://doi.org/10.1016/j.epsl.2010.07.024>.
- van Hinsbergen, D.J.J., Maffione, M., Plunder, A., Kaymakci, N., Ganerød, M., Hendriks, B.W.H., Corfu, F., Gürer, D., de Gelder, G.I.N.O., Peters, K., McPhee, P.J., Brouwer, F.M., Advokaat,

- E.L., and Vissers, R.L.M., 2016, Tectonic evolution and paleogeography of the Kırşehir block and the Central Anatolian ophiolites, Turkey (Intergovernmental Panel on Climate Change, Ed.): *Tectonics*, v. 35, p. 983–1014, <https://doi.org/10.1002/2015TC004018>.
- Vanacore, E.A., Taymaz, T., and Saygin, E., 2013, Moho structure of the Anatolian Plate from receiver function analysis: *Geophysics Journal International*, v. 193, p. 329–337, <https://doi.org/10.1093/gji/ggs107>.
- von Blanckenburg, F., and Davies, J.H., 1995, Slab breakoff: A model for syncollisional magmatism and tectonics in the Alps: *Tectonics*, v. 14, p. 120–131, <https://doi.org/10.1029/94TC02051>.
- Warren, L.M., Beck, S.L., Biryol, C.B., Zandt, G., Özacar, A.A., and Yang, Y., 2013, Crustal velocity structure of central and eastern Turkey from ambient noise tomography: *Geophysical Journal International*, v. 194, p. 1941–1954, <https://doi.org/10.1093/gji/ggt210>.
- Wortel, M.J.R., and Spakman, W., 2000, Subduction and slab detachment in the Mediterranean-Carpathian region: *Science*, v. 290, p. 1910–1917, <https://doi.org/10.1126/science.290.5498.1910>.
- Wu, J., Suppe, J., Lu, R., and Kanda, R., 2016, Philippine Sea and East Asian plate tectonics since 52 Ma constrained by new subducted slab reconstruction methods: *Journal of Geophysical Research–Solid Earth*, v. 121, p. 4670–4741, <https://doi.org/10.1002/2016JB012923>.
- Wysession, M.E., 1996, Imaging cold rock at the base of the mantle: The sometimes fate of slabs?, in Bebout, G.E., Scholl, D., Kirby, S., and Platt, J.P., eds., *Subduction Top to Bottom: American Geophysical Union Geophysical Monograph* 96, p. 369–384.
- Yanovskaya, T.B., Gobarenko, V.S., and Yegorova, T.P., 2016, Subcrustal structure of the Black Sea Basin from seismological data: *Izvestiya (Physics of the Solid Earth)*, v. 52, p. 14–28, <https://doi.org/10.1134/S1069351316010109>.
- Yegorova, T., Gobarenko, V., and Yanovskaya, T., 2013, Lithosphere structure of the Black Sea from 3-D gravity analysis and seismic tomography: *Geophysical Journal International*, v. 193, p. 287–303, <https://doi.org/10.1093/gji/ggs098>.
- Zhu, L., Mitchell, B.J., Akyol, N., Cemen, I., and Kekoali, K., 2006, Crustal thickness variations in the Aegean region and implications for the extension of continental crust: *Journal of Geophysical Research–Solid Earth*, v. 111, B01301, <https://doi.org/10.1029/2005JB003770>.
- Zitter, T.A.C., Woodside, J.M., and Mascle, J., 2003, The Anaximander Mountains: A clue to the tectonics of southwest Anatolia: *Geological Journal*, v. 38, p. 375–394, <https://doi.org/10.1002/gj.961>.
- Zor, E., 2008, Tomographic evidence of slab detachment beneath eastern Turkey and the Caucasus: *Geophysical Journal International*, v. 175, p. 1273–1282, <https://doi.org/10.1111/j.1365-246X.2008.03946.x>.